Author's personal copy

Inorganica Chimica Acta 363 (2010) 533-548



Contents lists available at ScienceDirect

Inorganica Chimica Acta

journal homepage: www.elsevier.com/locate/ica



Syntheses and structural analyses of chiral rhenium containing amines of the formula $(\eta^5-C_5H_5)Re(NO)(PPh_3)((CH_2)_nNRR')$ (n = 0, 1)

Sabine N. Seidel ^a, Markus Prommesberger ^a, Sandra Eichenseher ^a, Oliver Meyer ^b, Frank Hampel ^a, John A. Gladysz ^{a,b,c,*}

- ^a Institut für Organische Chemie and Interdisciplinary Center for Molecular Materials, Friedrich-Alexander-Universität Erlangen-Nürnberg, Henkestraße 42, 91054 Erlangen, Germany
- ^b Department of Chemistry, University of Utah, Salt Lake City, Utah 84112, USA
- ^c Department of Chemistry, Texas A&M University, P.O. Box 30012, College Station, Texas 77842-3012, USA

ARTICLE INFO

Article history: Received 3 February 2009 Accepted 28 March 2009 Available online 16 April 2009

Dedicated with affection to a long-time friend and fellow expatriate, Prof. Dr. Paul S. Pregosin

Keywords:
Rhenium
Amine complexes
Amido complexes
Ammonium ylide complexes
Hydrogen bonding
Crystal structures
Chiral complexes
Enantiopure complexes

ABSTRACT

The reaction of the racemic chiral methyl complex $(\eta^5-C_5H_5)Re(NO)(PPh_3)(CH_3)$ (1) with CF₃SO₃H and then NH₂CH₂C₆H₅ gives $[(\eta^5-C_5H_5)Re(NO)(PPh_3)(NH_2CH_2C_6H_5)]^+$ CF₃SO₃⁻ ([**4a**-H]⁺ CF₃SO₃⁻; 73%), and deprotonation with t-BuOK affords the amido complex $(\eta^5-C_5H_5)Re(NO)(PPh_3)(NHCH_2C_6H_5)$ (76%). Reactions of **1** with Ph₃C⁺ X⁻ and then primary or secondary amines give $[(\eta^5-C_5H_5)Re(NO)(PPh_3)(CH_2NHRR')]^+$ X⁻ ([**6**-H]⁺ X⁻; R/R'/X = a, $H/NH_2CH_2C_6H_5/BF_4$; a', $H/NH_2CH_2C_6H_5/PF_6$; b, $H/NH_2CH_2(CH_2)_2-CH_3/PF_6$; c, $H/(S)-NH_2CH(CH_3)C_6H_5/BF_4$); d, $CH_2CH_3/CH_2CH_3/PF_6$; e, $CH_2(CH_2)_2CH_3/CH_2(CH_2)_2CH_3/PF_6$; f, $CH_2C_6H_5/EF_6$; g, $-CH_2(CH_2)_2CH_2-PF_6$; h, $-CH_2(CH_2)_3CH_2-PF_6$; h, -C

 $\ensuremath{\text{@}}$ 2009 Elsevier B.V. All rights reserved.

1. Introduction

Amine ligands have played a key role in the development of coordination chemistry [1]. However, from the viewpoint of organic functional groups, amine complexes are more closely related to ammonium salts. Adducts of ammonia, primary amines, and secondary amines can often be deprotonated, with monocationic educts affording neutral species of the formula L_nMNRR' (I) [2–6]. These are frequently termed amido or amide complexes, and can be accessed by alternative pathways [2–9]. Amido complexes bear a closer relationship to organic amines, although in coordinatively unsaturated systems with sixteen or fewer metal valence electrons, multiple bonding involving the nitrogen lone pair is commonly found [10].

Coordinatively saturated amido complexes can be viewed as "metal-containing amines". In principle, amine functionality can be incorporated into other ligands, such as alkyl complexes of

E-mail address: gladysz@mail.chem.tamu.edu (J.A. Gladysz).

the formula $L_nM(CH_2)_{n'}NRR'$ (II) [11,12]. Given the immense utility of organic amines in catalysis, metal-containing amines would seem to hold considerable promise, particularly in view of the many chiral metal systems available. However, coordinatively saturated species are normally required to block chelation or oligomerization processes involving the nitrogen lone pair. Interestingly, amine centers that are α [2,3,5a,13] or β [11] to electronically saturated metal centers exhibit enhanced basicities and nucleophilicities.

In previous work, we have synthesized a number of coordinately saturated chiral-at-rhenium complexes of the formula $[(\eta^5\text{-}C_5H_5)Re(NO)(PPh_3)(NHRR')]^+\ X^-\ [4–9]$ and a few species $[(\eta^5\text{-}C_5H_5)Re(NO)(PPh_3)(CH_2NHRR')]^+\ X^-\ [11]$ in both racemic and enantiopure form. The latter can be termed ammonium ylide complexes [14]. These have been deprotonated to the corresponding rhenium containing amines $(\eta^5\text{-}C_5H_5)Re(NO)(PPh_3)(NRR')$ [5–10] and $(\eta^5\text{-}C_5H_5)Re(NO)(PPh_3)(CH_2NRR')$ [11], which are summarized in Chart 1. The former have also been accessed by nucleophilic additions to the cationic imine complexes [7–9], and are one of the few types of chiral-at-rhenium complexes that can undergo racemization at or slightly above room temperature. The

^{*} Corresponding author. Address: Department of Chemistry, Texas A&M University, P.O. Box 30012, College Station, Texas 77842-3012, USA.

Chart 1. Some rhenium containing amines reported earlier.

mechanism has been studied in detail [5b], and involves phosphine loss with anchimeric assistance from the nitrogen lone pair. In some cases this is followed by dimerization to give a doubly NRR′ bridged dirhenium complex [5a].

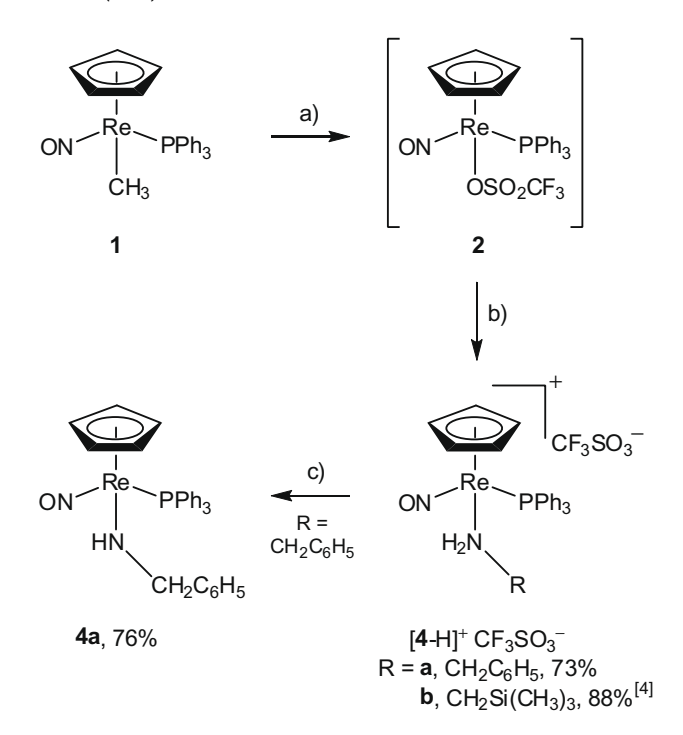
We have had a parallel interest in related rhenium containing phosphines, and particularly the use of enantiopure (η^5 - C_5H_5)Re(NO)(PPh₃)(CH₂PRR') systems to effect enantioselective phosphine catalyzed carbon–carbon bond forming reactions [15,16]. Since many of these transformations are also catalyzed by organic amines, it seemed logical to explore analogous reactions with rhenium containing amines. Towards this end, we revisited previously developed syntheses, particularly for ReCH₂NRR' species [11], and expanded them with regard to (a) skeletal diversity, (b) the types of stereogenic units present, and (c) additional functionality that may enhance catalysis. To help guide catalyst design, we also sought to enlarge the pool of crystallographically characterized complexes. These efforts are narrated below, and further details are available elsewhere [17].

2. Results

2.1. Syntheses of precursors

As shown in Scheme 1, the racemic or enantiopure methyl complex $(\eta^5\text{-}C_5H_5)\text{Re}(\text{NO})(\text{PPh}_3)(\text{CH}_3)$ (1) and $\text{CF}_3\text{SO}_3\text{H}$ rapidly react to give the triflate complex $(\eta^5\text{-}C_5H_5)\text{Re}(\text{NO})(\text{PPh}_3)(\text{OSO}_2\text{CF}_3)$ (2) [19]. The latter is one of several useful functional equivalents of the chiral sixteen-valence-electron rhenium Lewis acid $[(\eta^5\text{-}C_5H_5)\text{Re}(\text{NO})(\text{PPh}_3)]^+$, and readily combines with a variety of neutral Lewis bases D: to afford the triflate salts $[(\eta^5\text{-}C_5H_5)\text{Re}(\text{NO})(\text{PPh}_3)(\text{D})]^+$ CF_3SO_3^- [4,6,19]. Although 2 is isolable, it is most conveniently generated and used in situ. All steps proceed with a very high degree of retention at rhenium. Racemic and enantiopure 1 are in turn generated from commercial $\text{Re}_2(\text{CO})_{10}$ in a series of four or seven simple steps, and in 62% and 47% overall yields, respectively [20].

As shown in Scheme 2, racemic or enantiopure electrophilic methylidene complexes of the formula $[(\eta^5-C_5H_5)Re(-NO)(PPh_3)(=CH_2)]^+$ X^- ($\mathbf{3}^+$ X^-) can be generated by reactions of the hydride abstracting agents Ph_3C^+ X^- ($X^-=PF_6^-$, BF_4^-) and racemic or enantiopure $\mathbf{1}$ [21,22]. Although they can be isolated, they undergo novel disproportionations at room temperature [22]. Thus, neutral Lewis bases D: are added at low temperatures to give the cationic adducts $[(\eta^5-C_5H_5)Re(NO)(PPh_3)(CH_2D)]^+$ X^- [18,21,23]. All steps again proceed with retention of configuration at rhenium.



Scheme 1. Syntheses of complexes with rhenium-NH linkages. (a) CH_2CI_2 , CF_3SO_3H , 0 °C; (b) CH_2CI_2 , $NH_2CH_2C_6H_5$ or $NH_2CH_2Si(CH_3)_3$, 0 °C to room temperature; (c) THF, t-BuOK.

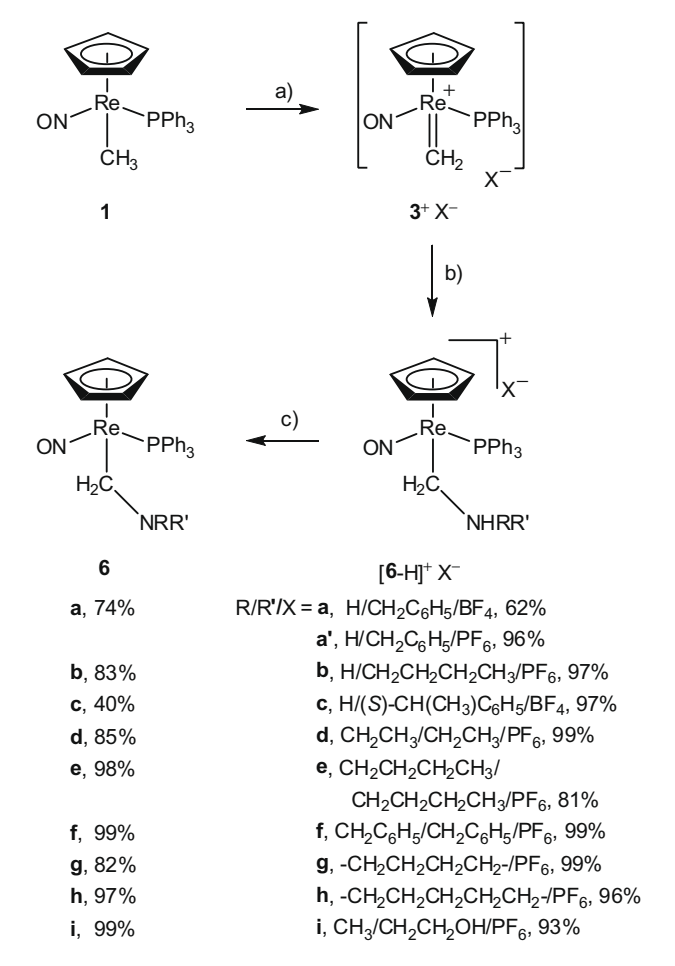
2.2. Rhenium containing amines of the formula (η^5 - C_5H_5)Re(NO)(PPh₃)(NHR)

Given the range of complexes in Chart 1, the need for additional examples was modest [4,5]. Thus, the triflate complex **2** was generated in situ and treated with benzyl amine (Scheme 1). Workup gave the amine complex $[(\eta^5-C_5H_5)Re(NO)(PPh_3)(NH_2CH_2C_6H_5)]^*$ CF₃SO₃ $^-$ ([**4a**-H]* CF₃SO₃ $^-$) in 73% yield. This analytically pure salt was characterized by IR and NMR (¹H, ¹³C, ³¹P) spectroscopy. All features were routine, and data are summarized in the experimental section.

Subsequent deprotonation with t-BuOK in THF gave the neutral amido compound (η^5 -C₅H₅)Re(NO)(PPh₃)(NHCH₂C₆H₅) (**4a**) in 76% yield after workup. However, this species was unstable in solution and the solid state, and was only characterized by 1 H and 31 P NMR. As noted above, related amido complexes undergo facile PPh₃ dissociation, which initiates various decomposition pathways.

Crystals of $[{\bf 4a}$ -H]⁺ CF₃SO₃⁻ were grown as described in the experimental section. Also, in the course of evaluating previously prepared amine complexes as precursors to amido complexes, crystals of the trimethylsilylmethyl amine complex $[(\eta^5-C_5H_5) \text{Re}(\text{NO})(\text{PPh}_3)(\text{NH}_2\text{CH}_2\text{Si}(\text{CH}_3)_3)]^+$ CF₃SO₃⁻ ($[{\bf 4b}$ -H]⁺ CF₃SO₃⁻) [4] were obtained. Only one other compound in this series, the dimethyl amine complex $[(\eta^5-C_5H_5)\text{Re}(\text{NO})(\text{PPh}_3)(\text{NH}(\text{CH}_3)_2)]^+$ CF₃SO₃⁻ ($[{\bf 5}$ -H]⁺ CF₃SO₃⁻), had been structurally characterized. Accordingly, the crystal structures of $[{\bf 4a}$,b-H]⁺ CF₃SO₃⁻ were determined as summarized in Table 1 and the experimental section.

The molecular structures of [**4a,b**-H]⁺ CF₃SO₃⁻ are depicted in Fig. 1, together with Newman type projections down the N-Re bonds. Two independent molecules of [**4b**-H]⁺ CF₃SO₃⁻ were present, but the cations exhibited very similar conformations, as reflected by the close correspondence of torsion angles. Metrical parameters are summarized in Table 2. For reference, a Newman projection of [**5**-H]⁺ CF₃SO₃⁻ is also provided in Fig. 1 (bottom). Hydrogen bonding between the triflate anion and an NH bond of



Scheme 2. Syntheses of racemic rhenium containing secondary and tertiary amines **6a–i.** (a) CH_2CI_2 , Ph_3C^+ X^- , -78 °C; (b) CH_2CI_2 , NHRR', -78 °C to room temperature; (c) THF, t-BuOK.

the cation (CF₃SO₂O···H···NRR'Re) was evident in each case. The shortest $\mathbf{O} \cdot \cdot H \cdot \cdot \mathbf{N}$ and $\mathbf{O} \cdot \cdot H$ distances (as derived from calculated hydrogen positions) were 2.953 Å and 2.055 Å in [$\mathbf{4a}$ -H] $^+$ CF₃SO₃ $^-$, 2.864 Å and 1.953 Å in [$\mathbf{4b}$ -H] $^+$ CF₃SO₃ $^-$, and 3.06 Å and 2.37 Å for [$\mathbf{5}$ -H] $^+$ CF₃SO₃ $^-$. The structures of the cations are further compared in the discussion section.

2.3. Secondary rhenium containing amines of the formula (η^5 - C_5H_5)Re(NO)(PPh₃)(CH₂NHR)

As shown in Scheme 2, the methylidene complex ${\bf 3}^+$ X $^-$ was generated in situ and treated with the primary amines (${\bf a}$) benzyl amine, (${\bf b}$) n-butyl amine, or (${\bf c}$) (S)-1-phenylethylamine. The mixtures were allowed to warm to room temperature, and workups gave the ammonium ylide complexes $[(\eta^5-C_5H_5)Re(NO)(PPh_3)-(CH_2NH_2R)]^+$ X $^-$ ([${\bf 6}$ -H] $^+$ X $^-$; R/X = ${\bf a}$, NH₂CH₂C₆H₅/BF₄; ${\bf a}'$, NH₂CH₂C₆H₅/PF₆; ${\bf b}$, NH₂CH₂CH₂CH₂CH₃/PF₆; ${\bf c}$, (S)-NH₂CH(CH₃)-C₆H₅/BF₄) in 63–99% yields as analytically pure yellow powders.

The complexes $[\mathbf{6a-c}-H]^+$ X^- were indefinitely stable as solids, but showed some decomposition after brief periods in CDCl₃. Thus, NMR spectra were recorded in CD₂Cl₂, and data are summarized in the experimental section. In the case of $[\mathbf{6c}-H]^+$ BF₄ $^-$, two sets of signals, corresponding to the $R_{Re}S_C$ and $S_{Re}S_C$ diastereomers, were apparent (52:48).

The salts [**6a-c**-H]⁺ X⁻ were subsequently deprotonated with t-BuOK in THF at room temperature. As summarized in Scheme 2, workups gave the neutral amido complexes (η^5 -C₅H₅) Re(NO)(PPh₃)(CH₂NHR) (**6a-c**) in 40–83% yields and 95–99% puri-

ties (^{31}P NMR). These were characterized analogously to [**6a-c**-H]⁺ X⁻. However, unlike their tertiary amine analogs (below), they decomposed in solution (**6a,c** > **6b**). In the case of **6c**, two diastereomers were again apparent.

Several trends were evident in the spectroscopic data. The cyclopentadienyl ^1H NMR signals of 6a-c (δ 4.67–4.83) were upfield of those of $[\textbf{6a-c-H}]^+$ X $^-$ (δ 5.11–5.39), but the ^{13}C NMR signals showed little difference (d 89.9–90.3 versus δ 90.9–91.6). The ^{31}P NMR signals showed the opposite trend (6a-c, d 25.0–27.2; $[\textbf{6a-c-H}]^+$ X $^-$, δ 21.0–22.4). The ReCH₂N ^{13}C NMR signal of $[\textbf{6b-H}]^+$ PF $_6^-$ (δ 27.9) was considerably downfield of those of the other cations (δ 20.0–18.7), all of which have an N-benzyl group. The IR ν_{NO} values of 6a-c (1613–1617 cm $^{-1}$) were at lower frequencies than those of $[\textbf{6a-c-H}]^+$ X $^-$ (1633–1660 cm $^{-1}$). This indicates, as also suggested the ^1H NMR data, that the rhenium centers of the neutral complexes are somewhat more electron rich.

As shown in Scheme 3, the sequence with (S)-NH₂CH(CH₃)C₆H₅ was repeated starting with the enantiopure rhenium methyl complex (R)-1 [20,24]. As expected, this gave the enantiopure amine complex $(R_{Re}S_C)$ -[$\mathbf{6c}$ -H] $^+$ BF $_4$ $^-$ (77%). The sample was treated with t-BuOK in THF analogously to the diastereomer mixture above. After solvent removal, the crude $(R_{Re}S_C)$ - $\mathbf{6c}$ was extracted with benzene, and the extract was filtered through Celite. The solvent was again removed and various crystallization conditions assayed. Orange crystals were obtained from CH₂Cl₂/pentane.

Prisms of a solvate of $[\mathbf{6a'}-\mathbf{H}]^+$ PF₆ $^-$ were obtained as described in the experimental section. The crystal structures of $[\mathbf{6a'}-\mathbf{H}]^+$ PF₆ $^-$ and $(R_{Re}S_C)$ - $\mathbf{6c}$ were determined as for the other complexes above. The molecular structures are shown in Fig. 2, with the configuration of the latter (confirmed by Flack's test) *inverted* such that the rhenium configuration corresponds to that shown for the racemates (and other racemic and enantiopure compounds in previous papers in this series). Metrical parameters are summarized in Table 3. Hydrogen bonding between the hexafluorophosphate anion and ReCH₂NH₂ protons was evident in $[\mathbf{6a'}$ - $\mathbf{H}]^+$ PF₆ $^-$, and the shortest $\mathbf{F} \cdots \mathbf{H}$ and $\mathbf{F} \cdots \mathbf{N}$ contacts are incorporated into Table 3. These values are well within the range of other hydrogen bonds between hexafluorophosphate anions and NH protons of cations [25].

2.4. Tertiary rhenium containing amines of the formula $(\eta^5$ -C₅H₅)Re(NO)(PPh₃)(CH₂NRR')

As shown in Scheme 2, the methylidene complex ${\bf 3}^+$ PF $_6^-$ was similarly treated with the secondary amines (${\bf d}$) diethyl amine, (${\bf e}$) di-n-butyl amine, (${\bf f}$) dibenzyl amine, (${\bf g}$) pyrrolidine, (${\bf h}$) piperidine, or (${\bf i}$) methyl 2-hydroxyethyl amine. Workups gave the ylide complexes $[(\eta^5-C_5H_5)Re(NO)(PPh_3)(CH_2NHRR')]^+$ PF $_6^-$ ([${\bf 6}$ -H] $^+$ PF $_6^-$; R/R' = ${\bf d}$, (CH $_2$ CH $_3$) $_2$; ${\bf e}$, (CH $_2$ CH $_2$ CH $_2$ CH $_3$) $_2$; ${\bf f}$, (CH $_2$ CH $_3$) $_2$; ${\bf g}$, -CH $_2$ CH $_3$) $_3$; ${\bf f}$, (CH $_3$ CH $_3$ C

The salts $[\mathbf{6d}\text{-i-H}]^+$ PF_6^- were similarly deprotonated with t-BuOK in THF at room temperature. Workups gave the corresponding analytically pure neutral complexes $(\eta^5\text{-}C_5H_5)\text{-Re}(NO)(PPh_3)(CH_2NRR')$ $(\mathbf{6d}\text{-i})$ in 85-99% yields. These were characterized analogously to the other new complexes above. In the case of $\mathbf{6i}$, two diastereomers were no longer apparent, consistent with the expected rapid pyramidal inversion at nitrogen. The spectroscopic properties of $[\mathbf{6d}\text{-i-H}]^+$ PF_6^- and $\mathbf{6d}\text{-i}$ were similar to those of their primary amine derived analogs in the previous section. However, these complexes were much more robust in solution.

Table 1 Summary of crystallographic data.^a

	[4a -H] ⁺ CF ₃ SO ₃ ⁻	[4b -H] ⁺ CF ₃ SO ₃ ⁻	$[\mathbf{6a'} - \mathbf{H}]^+ PF_6^- \cdot (CH_2Cl_2)_{0.5} \cdot (C_6H_6)_{0.5}$	$(R_{\text{Re}}S_{\text{C}})$ - 6c
Empirical formula	$C_{31}H_{29}F_3N_2O_4PReS$	$C_{32}H_{31}F_3N_2O_4PReS$	$C_{34.50}H_{35}CIF_6N_2OP_2Re$	$C_{32}H_{32}N_2OPRe$
Formula weight	799.79	813.82	891.24	677.77
Crystal system	triclinic	triclinic	triclinic	orthorhombic
Space group	ΡĪ	ΡĪ	ΡĪ	$P2_12_12_1$
Unit cell dimensions:	0.2001(2)	10.0257(2)	11 (04/2)	0.0002(10)
a (Å)	9.2091(2)	10.9357(2)	11.694(2)	9.0902(18)
b (Å) c (Å)	11.1277(3)	12.6353(2)	12.392(3)	9.753(2)
α (°)	16.2055(2)	12.9541(3)	13.975(3) 92.89(3)	31.266(6) 90
β(°)	105.008(1) 90.690(1)	97.372(1) 101.502(1)	113.33(3)	90
γ(°)	106.710(1)	114.504(1)	106.40(3)	90
V (Å ³)	1529.56(6)	1550.68(5)	1753.5(6)	2772.1(10)
Z	2	2	2	4
ρ calcd (Mgm ⁻³)	1.737	1.743	1.688	1.624
$\mu (\text{mm}^{-1})$	4.150	4.095	3.695	4.469
F(000)	788	804	880	1344
Crystal size (mm³)	$0.15 \times 0.10 \times 0.10$	$0.20 \times 0.20 \times 0.10$	$0.30 \times 0.20 \times 0.20$	$0.40 \times 0.30 \times 0.30$
Θ range	2.32 to 27.54	2.13 to 27.51	1.97 to 27.51	2.46 to 26.28
Index ranges (h, k, l)	-11,11; -14,14; -21,20	-14,14; -16,16; -16,16	-15,15; -16,16; -18,18	-11,11; -12,12; -38,38
Reflections collected	13258	13445	15631	6408
Independent reflections	7004	7099	8059	5615
R _{int}	0.0212	0.0167	0.0233	0.0514
Reflections $[I > 2\sigma(I)]$	6315	6535	7157	4706
Completeness to Θ	99.5% (27.5)	99.6%	99.9% (27.51)	99.9% (27.5)
Data/restraints/parameters	7004/0/388	7099/6/398	8059/0/433	5615/0/334
Goodness-of-fit on F^2	1.052	1.029	1.026	1.083
R indices (final) $[I > 2\sigma(I)]$				
R_1	0.0255	0.0362	0.0303	0.0418
wR ₂	0.0571	0.0942	0.0772	0.0810
R indices (all data)				
R_1	0.0308	0.0402	0.0373	0.0625
wR ₂	0.0591	0.0969	0.0808	0.0916
Largest difference peak/hole (eÅ ⁻³)	1.635/-0.974	2.743/-1.414	1.886/-1.695	0.886/-0.863
	[6d-H] ⁺ PF ₆ ⁻ -CH ₂ Cl ₂	[6f -H] ⁺ PF ₆ - ·(CH ₂ Cl ₂) _{1.5}	6f	[6h -H] ⁺ PF ₆ - ·CH ₂ Cl ₂
Empirical formula	$C_{29}H_{35}Cl_2F_6N_2OP_2Re$	$C_{39,50}H_{41}Cl_3F_6N_2OP_2Re$	C ₃₈ H ₃₆ N ₂ OPRe	$C_{30}H_{35}Cl_2F_6N_2OP_2Re$
Formula weight	860.63	1028.23	753.86	872.64
<u> </u>				
Crystal system	triclinic	triclinic		
Crystal system	triclinic Pī	triclinic pī	monoclinic	triclinic pī
Space group	triclinic PĪ	triclinic PĪ	P2 ₁ /n	PĪ
Space group Unit cell dimensions:	ΡĪ	ΡĪ	P2 ₁ /n	PĪ
Space group Unit cell dimensions: a (Å)	PĪ 9.2814(2)	PĪ 11.0420(2)	P2 ₁ /n 13.8657(1)	PĪ 9.4257(2)
Space group Unit cell dimensions: a (Å) b (Å)	PĪ 9.2814(2) 13.7840(3)	PĪ 11.0420(2) 13.1712(3)	P2 ₁ /n 13.8657(1) 15.8282(1)	PĪ 9.4257(2) 13.8256(3)
Space group Unit cell dimensions: a (Å) b (Å) c (Å)	PĪ 9.2814(2) 13.7840(3) 14.0177(2)	PĪ 11.0420(2) 13.1712(3) 15.4282(3)	P2 ₁ /n 13.8657(1) 15.8282(1) 14.9035(1)	PĪ 9.4257(2) 13.8256(3) 13.9046(3)
Space group Unit cell dimensions: a (Å) b (Å) c (Å) α (°)	P1 9.2814(2) 13.7840(3) 14.0177(2) 83.819(1)	PĪ 11.0420(2) 13.1712(3) 15.4282(3) 83.220(1)	P2 ₁ /n 13.8657(1) 15.8282(1) 14.9035(1) 90	PĪ 9.4257(2) 13.8256(3) 13.9046(3) 83.678(1)
Space group Unit cell dimensions: a (Å) b (Å) c (Å) c (Å) c (Å) c (b	PĪ 9.2814(2) 13.7840(3) 14.0177(2) 83.819(1) 72.394(1)	PĪ 11.0420(2) 13.1712(3) 15.4282(3) 83.220(1) 86.225(1)	P2 ₁ /n 13.8657(1) 15.8282(1) 14.9035(1) 90 99.440(2)	PĪ 9.4257(2) 13.8256(3) 13.9046(3) 83.678(1) 71.495(1)
Space group Unit cell dimensions: a (Å) b (Å) c (Å) c (Å) c (c (c (c)) c (c) c (c) c (c) c (c)	P1 9.2814(2) 13.7840(3) 14.0177(2) 83.819(1) 72.394(1) 73.658(1)	PĪ 11.0420(2) 13.1712(3) 15.4282(3) 83.220(1) 86.225(1) 66.887(1)	P2 ₁ /n 13.8657(1) 15.8282(1) 14.9035(1) 90 99.440(2)	PĪ 9.4257(2) 13.8256(3) 13.9046(3) 83.678(1) 71.495(1) 74.952(1)
Space group Unit cell dimensions: a (Å) b (Å) c (Å) c (Å) c (c (Å) c (c (Å) c (c	P1 9.2814(2) 13.7840(3) 14.0177(2) 83.819(1) 72.394(1) 73.658(1) 1639.79(6)	PĪ 11.0420(2) 13.1712(3) 15.4282(3) 83.220(1) 86.225(1) 66.887(1) 2048.82(7)	P2 ₁ /n 13.8657(1) 15.8282(1) 14.9035(1) 90 99.440(2) 90 3226.56(4)	PĪ 9.4257(2) 13.8256(3) 13.9046(3) 83.678(1) 71.495(1) 74.952(1) 1658.62(6)
Space group Unit cell dimensions: a (Å) b (Å) c (Å) c (Å) c (Å) c (c (Å) c (c	P1 9.2814(2) 13.7840(3) 14.0177(2) 83.819(1) 72.394(1) 73.658(1) 1639.79(6) 2	PĪ 11.0420(2) 13.1712(3) 15.4282(3) 83.220(1) 86.225(1) 66.887(1) 2048.82(7) 2	P2 ₁ /n 13.8657(1) 15.8282(1) 14.9035(1) 90 99.440(2) 90 3226.56(4) 4	PĪ 9.4257(2) 13.8256(3) 13.9046(3) 83.678(1) 71.495(1) 74.952(1) 1658.62(6) 2
Space group Unit cell dimensions: a (Å) b (Å) c (Å) α (°) β (°) β (°) γ	P1 9.2814(2) 13.7840(3) 14.0177(2) 83.819(1) 72.394(1) 73.658(1) 1639.79(6) 2 1.743	PĪ 11.0420(2) 13.1712(3) 15.4282(3) 83.220(1) 86.225(1) 66.887(1) 2048.82(7) 2 1.667	P2 ₁ /n 13.8657(1) 15.8282(1) 14.9035(1) 90 99.440(2) 90 3226.56(4) 4 1.552	PĪ 9.4257(2) 13.8256(3) 13.9046(3) 83.678(1) 71.495(1) 74.952(1) 1658.62(6) 2 1.747
Space group Unit cell dimensions: a (Å) b (Å) c (Å) a (°) a	P1 9.2814(2) 13.7840(3) 14.0177(2) 83.819(1) 72.394(1) 73.658(1) 1639.79(6) 2 1.743 4.026	PĪ 11.0420(2) 13.1712(3) 15.4282(3) 83.220(1) 86.225(1) 66.887(1) 2048.82(7) 2 1.667 3.301	P2 ₁ /n 13.8657(1) 15.8282(1) 14.9035(1) 90 99.440(2) 90 3226.56(4) 4 1.552 3.848	PĪ 9.4257(2) 13.8256(3) 13.9046(3) 83.678(1) 71.495(1) 74.952(1) 1658.62(6) 2 1.747 3.982
Space group Unit cell dimensions: a (Å) b (Å) c (Å) a (°) a	PĪ 9.2814(2) 13.7840(3) 14.0177(2) 83.819(1) 72.394(1) 73.658(1) 1639.79(6) 2 1.743 4.026 848	PĪ 11.0420(2) 13.1712(3) 15.4282(3) 83.220(1) 86.225(1) 66.887(1) 2048.82(7) 2 1.667 3.301 1020	P2 ₁ /n 13.8657(1) 15.8282(1) 14.9035(1) 90 99.440(2) 90 3226.56(4) 4 1.552 3.848 1504	P1 9.4257(2) 13.8256(3) 13.9046(3) 83.678(1) 71.495(1) 74.952(1) 1658.62(6) 2 1.747 3.982 860
Space group Unit cell dimensions: a (Å) b (Å) c (Å) a (°) b	$P\bar{1}$ 9.2814(2) 13.7840(3) 14.0177(2) 83.819(1) 72.394(1) 73.658(1) 1639.79(6) 2 1.743 4.026 848 0.20 × 0.20 × 0.10	Pī 11.0420(2) 13.1712(3) 15.4282(3) 83.220(1) 86.225(1) 66.887(1) 2048.82(7) 2 1.667 3.301 1020 0.15 × 0.15 × 0.15	P2 ₁ /n 13.8657(1) 15.8282(1) 14.9035(1) 90 99.440(2) 90 3226.56(4) 4 1.552 3.848 1504 0.10 × 0.10 × 0.10	P1 9.4257(2) 13.8256(3) 13.9046(3) 83.678(1) 71.495(1) 74.952(1) 1658.62(6) 2 1.747 3.982 860 0.10 × 0.10 × 0.10
Space group Unit cell dimensions: a (Å) b (Å) c (Å) c (Å) c (Å) c (Å) c (d) d (d) d) d (d) d) d (d) d) d 0	P1 9.2814(2) 13.7840(3) 14.0177(2) 83.819(1) 72.394(1) 73.658(1) 1639.79(6) 2 1.743 4.026 848 0.20 × 0.20 × 0.10 2.14 to 27.48	Pī 11.0420(2) 13.1712(3) 15.4282(3) 83.220(1) 86.225(1) 66.887(1) 2048.82(7) 2 1.667 3.301 1020 0.15 × 0.15 × 0.15 2.06 to 27.50	P2 ₁ /n 13.8657(1) 15.8282(1) 14.9035(1) 90 99.440(2) 90 3226.56(4) 4 1.552 3.848 1504 0.10 × 0.10 × 0.10 2.26 to 27.51	P1 9.4257(2) 13.8256(3) 13.9046(3) 83.678(1) 71.495(1) 74.952(1) 1658.62(6) 2 1.747 3.982 860 0.10 × 0.10 × 0.10 2.39 to 27.51
Space group Unit cell dimensions: a (Å) b (Å) c (Å) c (Å) c (Å) c (Å) c (c (c (Å) c (c	$P\bar{1}$ 9.2814(2) 13.7840(3) 14.0177(2) 83.819(1) 72.394(1) 73.658(1) 1639.79(6) 2 1.743 4.026 848 0.20 × 0.20 × 0.10 2.14 to 27.48 -12,12; -17,17; -18,18	Pī 11.0420(2) 13.1712(3) 15.4282(3) 83.220(1) 86.225(1) 66.887(1) 2048.82(7) 2 1.667 3.301 1020 0.15 × 0.15 × 0.15	$P2_1/n$ 13.8657(1) 15.8282(1) 14.9035(1) 90 99.440(2) 90 3226.56(4) 4 1.552 3.848 1504 0.10 × 0.10 × 0.10 2.26 to 27.51 -17,18; -20,19; -19,19	P1 9.4257(2) 13.8256(3) 13.9046(3) 83.678(1) 71.495(1) 74.952(1) 1658.62(6) 2 1.747 3.982 860 0.10 × 0.10 × 0.10 2.39 to 27.51 -12,12; -17,17; -18,18
Space group Unit cell dimensions: a (Å) b (Å) c (Å) c (Å) c (Å) c (Å) c (c	$P\bar{1}$ 9.2814(2) 13.7840(3) 14.0177(2) 83.819(1) 72.394(1) 73.658(1) 1639.79(6) 2 1.743 4.026 848 0.20 × 0.20 × 0.10 2.14 to 27.48 -12,12; -17,17; -18,18 14180	$P\bar{1}$ 11.0420(2) 13.1712(3) 15.4282(3) 83.220(1) 86.225(1) 66.887(1) 2048.82(7) 2 1.667 3.301 1020 0.15 × 0.15 × 0.15 2.06 to 27.50 -14,14; -16,17; -20,20 17381	$P2_1/n$ 13.8657(1) 15.8282(1) 14.9035(1) 90 99.440(2) 90 3226.56(4) 4 1.552 3.848 1504 0.10 × 0.10 × 0.10 2.26 to 27.51 -17,18; -20,19; -19,19 13276	$P\bar{1}$ 9.4257(2) 13.8256(3) 13.9046(3) 83.678(1) 71.495(1) 74.952(1) 1658.62(6) 2 1.747 3.982 860 0.10 × 0.10 × 0.10 2.39 to 27.51 -12,12; -17,17; -18,18
Space group Unit cell dimensions: a (Å) b (Å) c (Å) a (°) a	$P\bar{1}$ 9.2814(2) 13.7840(3) 14.0177(2) 83.819(1) 72.394(1) 73.658(1) 1639.79(6) 2 1.743 4.026 848 0.20 × 0.20 × 0.10 2.14 to 27.48 -12,12; -17,17; -18,18	Pī 11.0420(2) 13.1712(3) 15.4282(3) 83.220(1) 86.225(1) 66.887(1) 2048.82(7) 2 1.667 3.301 1020 0.15 × 0.15 × 0.15 2.06 to 27.50 -14,14; -16,17; -20,20	$P2_1/n$ 13.8657(1) 15.8282(1) 14.9035(1) 90 99.440(2) 90 3226.56(4) 4 1.552 3.848 1504 0.10 × 0.10 × 0.10 2.26 to 27.51 -17,18; -20,19; -19,19	P1 9.4257(2) 13.8256(3) 13.9046(3) 83.678(1) 71.495(1) 74.952(1) 1658.62(6) 2 1.747 3.982 860 0.10 × 0.10 × 0.10 2.39 to 27.51 -12,12; -17,17; -18,18
Space group Unit cell dimensions: a (Å) b (Å) c (Å) c (Å) c (Å) c (Å) c (c	P1 9.2814(2) 13.7840(3) 14.0177(2) 83.819(1) 72.394(1) 73.658(1) 1639.79(6) 2 1.743 4.026 848 0.20 × 0.20 × 0.10 2.14 to 27.48 -12,12; -17,17; -18,18 14180 7479	Pī 11.0420(2) 13.1712(3) 15.4282(3) 83.220(1) 86.225(1) 66.887(1) 2048.82(7) 2 1.667 3.301 1020 0.15 × 0.15 × 0.15 2.06 to 27.50 -14,14; -16,17; -20,20 17381 9226	$P2_1/n$ 13.8657(1) 15.8282(1) 14.9035(1) 90 99.440(2) 90 3226.56(4) 4 1.552 3.848 1504 0.10 × 0.10 × 0.10 2.26 to 27.51 -17,18; -20,19; -19,19 13276 7410	P1 9.4257(2) 13.8256(3) 13.9046(3) 83.678(1) 71.495(1) 74.952(1) 1658.62(6) 2 1.747 3.982 860 0.10 × 0.10 × 0.10 2.39 to 27.51 -12,12; -17,17; -18,18 14386 7589
Space group Unit cell dimensions: a (A) b (A) c (A)	$P\bar{1}$ 9.2814(2) 13.7840(3) 14.0177(2) 83.819(1) 72.394(1) 73.658(1) 1639.79(6) 2 1.743 4.026 848 0.20 × 0.20 × 0.10 2.14 to 27.48 -12,12; -17,17; -18,18 14180 7479 0.0191	Pī 11.0420(2) 13.1712(3) 15.4282(3) 83.220(1) 86.225(1) 66.887(1) 2048.82(7) 2 1.667 3.301 1020 0.15 × 0.15 × 0.15 2.06 to 27.50 -14,14; -16,17; -20,20 17381 9226 0.0205 8272	$P2_1/n$ 13.8657(1) 15.8282(1) 14.9035(1) 90 99.440(2) 90 3226.56(4) 4 1.552 3.848 1504 0.10 × 0.10 × 0.10 2.26 to 27.51 -17.18; -20,19; -19,19 13276 7410 0.0274 5526	P1 9.4257(2) 13.8256(3) 13.9046(3) 83.678(1) 71.495(1) 74.952(1) 1658.62(6) 2 1.747 3.982 860 0.10 × 0.10 × 0.10 2.39 to 27.51 -12,12; -17,17; -18,18 14386 7589 0.0215 6820
Space group Unit cell dimensions: a (Å) b (Å) c (Å) a (°) a	$P\bar{1}$ 9.2814(2) 13.7840(3) 14.0177(2) 83.819(1) 72.394(1) 73.658(1) 1639.79(6) 2 1.743 4.026 848 0.20 × 0.20 × 0.10 2.14 to 27.48 -12,12; -17,17; -18,18 14180 7479 0.0191 6833	Pī 11.0420(2) 13.1712(3) 15.4282(3) 83.220(1) 86.225(1) 66.887(1) 2048.82(7) 2 1.667 3.301 1020 0.15 × 0.15 × 0.15 2.06 to 27.50 -14,14; -16,17; -20,20 17381 9226 0.0205	$P2_1/n$ 13.8657(1) 15.8282(1) 14.9035(1) 90 99.440(2) 90 3226.56(4) 4 1.552 3.848 1504 0.10 × 0.10 × 0.10 2.26 to 27.51 -17.18; -20,19; -19,19 13276 7410 0.0274	P1 9.4257(2) 13.8256(3) 13.9046(3) 83.678(1) 71.495(1) 74.952(1) 1658.62(6) 2 1.747 3.982 860 0.10 × 0.10 × 0.10 2.39 to 27.51 -12,12; -17,17; -18,18 14386 7589 0.0215 6820 99.5% (27.5)
Space group Unit cell dimensions: a (Å) b (Å) c	$P\bar{1}$ 9.2814(2) 13.7840(3) 14.0177(2) 83.819(1) 72.394(1) 73.658(1) 1639.79(6) 2 1.743 4.026 848 0.20 × 0.20 × 0.10 2.14 to 27.48 -12,12; -17,17; -18,18 14180 7479 0.0191 6833 99.4% (27.5)	Pī 11.0420(2) 13.1712(3) 15.4282(3) 83.220(1) 86.225(1) 66.887(1) 2048.82(7) 2 1.667 3.301 1020 0.15 × 0.15 × 0.15 2.06 to 27.50 -14,14; -16,17; -20,20 17381 9226 0.0205 8272 98.0% (27.5)	$P2_1/n$ 13.8657(1) 15.8282(1) 14.9035(1) 90 99.440(2) 90 3226.56(4) 4 1.552 3.848 1504 0.10 × 0.10 × 0.10 2.26 to 27.51 -17,18; -20,19; -19,19 13276 7410 0.0274 5526 99.8% (27.5)	P1 9.4257(2) 13.8256(3) 13.9046(3) 83.678(1) 71.495(1) 74.952(1) 1658.62(6) 2 1.747 3.982 860 0.10 × 0.10 × 0.10 2.39 to 27.51 -12,12; -17,17; -18,18 14386 7589 0.0215 6820
Space group Unit cell dimensions: a (Å) b (Å) c (Å) c (Å) c (Å) c (Å) c (Å) c (c (c (Å) c (c	$P\bar{1}$ 9.2814(2) 13.7840(3) 14.0177(2) 83.819(1) 72.394(1) 73.658(1) 1639.79(6) 2 1.743 4.026 848 0.20 × 0.20 × 0.10 2.14 to 27.48 -12,12; -17,17; -18,18 14180 7479 0.0191 6833 99.4% (27.5) 7479/0/389	Pī 11.0420(2) 13.1712(3) 15.4282(3) 83.220(1) 86.225(1) 66.887(1) 2048.82(7) 2 1.667 3.301 1020 0.15 × 0.15 × 0.15 2.06 to 27.50 -14,14; -16,17; -20,20 17381 9226 0.0205 8272 98.0% (27.5) 9226/3/498	$P2_1/n$ 13.8657(1) 15.8282(1) 14.9035(1) 90 99.440(2) 90 3226.56(4) 4 1.552 3.848 1504 0.10 × 0.10 × 0.10 2.26 to 27.51 -17,18; -20,19; -19,19 13276 7410 0.0274 5526 99.8% (27.5) 7410/0/389	P1 9.4257(2) 13.8256(3) 13.9046(3) 83.678(1) 71.495(1) 74.952(1) 1658.62(6) 2 1.747 3.982 860 0.10 × 0.10 × 0.10 2.39 to 27.51 -12,12; -17,17; -18,18 14386 7589 0.0215 6820 99.5% (27.5) 7589/6/407
Space group Unit cell dimensions: a (Å) b (Å) c (Å) a (°) a	P1 9.2814(2) 13.7840(3) 14.0177(2) 83.819(1) 72.394(1) 73.658(1) 1639.79(6) 2 1.743 4.026 848 0.20 × 0.20 × 0.10 2.14 to 27.48 -12,12; -17,17; -18,18 14180 7479 0.0191 6833 99.4% (27.5) 7479/0/389 1.055	Pī 11.0420(2) 13.1712(3) 15.4282(3) 83.220(1) 86.225(1) 66.887(1) 2048.82(7) 2 1.667 3.301 1020 0.15 × 0.15 × 0.15 2.06 to 27.50 -14,14; -16,17; -20,20 17381 9226 0.0205 8272 98.0% (27.5) 9226/3/498 1.070	$P2_1/n$ 13.8657(1) 15.8282(1) 14.9035(1) 90 99.440(2) 90 3226.56(4) 4 1.552 3.848 1504 0.10 × 0.10 × 0.10 2.26 to 27.51 -17,18; -20,19; -19,19 13276 7410 0.0274 5526 99.8% (27.5) 7410/0/389 1.000	P1 9.4257(2) 13.8256(3) 13.9046(3) 83.678(1) 71.495(1) 74.952(1) 1658.62(6) 2 1.747 3.982 860 0.10 × 0.10 × 0.10 2.39 to 27.51 -12,12; -17,17; -18,18 14386 7589 0.0215 6820 99.5% (27.5) 7589/6/407 1.045
Space group Unit cell dimensions: a (Å) b (Å) c (Å) a (°) a	Pī 9.2814(2) 13.7840(3) 14.0177(2) 83.819(1) 72.394(1) 73.658(1) 1639.79(6) 2 1.743 4.026 848 0.20 × 0.20 × 0.10 2.14 to 27.48 -12,12; -17,17; -18,18 14180 7479 0.0191 6833 99.4% (27.5) 7479/0/389 1.055 0.0239	Pī 11.0420(2) 13.1712(3) 15.4282(3) 83.220(1) 86.225(1) 66.887(1) 2048.82(7) 2 1.667 3.301 1020 0.15 × 0.15 × 0.15 2.06 to 27.50 -14,14; -16,17; -20,20 17381 9226 0.0205 8272 98.0% (27.5) 9226/3/498 1.070 0.0394	$P2_1/n$ 13.8657(1) 15.8282(1) 14.9035(1) 90 99.440(2) 90 3226.56(4) 4 1.552 3.848 1504 0.10 × 0.10 × 0.10 2.26 to 27.51 -17.18; -20,19; -19,19 13276 7410 0.0274 5526 99.8% (27.5) 7410/0/389 1.000 0.0298	P1 9.4257(2) 13.8256(3) 13.9046(3) 83.678(1) 71.495(1) 74.952(1) 1658.62(6) 2 1.747 3.982 860 0.10 × 0.10 × 0.10 2.39 to 27.51 -12,12; -17,17; -18,18 14386 7589 0.0215 6820 99.5% (27.5) 7589/6/407 1.045 0.0329
Space group Unit cell dimensions: a (A) b (A) c (A)	P1 9.2814(2) 13.7840(3) 14.0177(2) 83.819(1) 72.394(1) 73.658(1) 1639.79(6) 2 1.743 4.026 848 0.20 × 0.20 × 0.10 2.14 to 27.48 -12,12; -17,17; -18,18 14180 7479 0.0191 6833 99.4% (27.5) 7479/0/389 1.055	Pī 11.0420(2) 13.1712(3) 15.4282(3) 83.220(1) 86.225(1) 66.887(1) 2048.82(7) 2 1.667 3.301 1020 0.15 × 0.15 × 0.15 2.06 to 27.50 -14,14; -16,17; -20,20 17381 9226 0.0205 8272 98.0% (27.5) 9226/3/498 1.070	$P2_1/n$ 13.8657(1) 15.8282(1) 14.9035(1) 90 99.440(2) 90 3226.56(4) 4 1.552 3.848 1504 0.10 × 0.10 × 0.10 2.26 to 27.51 -17,18; -20,19; -19,19 13276 7410 0.0274 5526 99.8% (27.5) 7410/0/389 1.000	P1 9.4257(2) 13.8256(3) 13.9046(3) 83.678(1) 71.495(1) 74.952(1) 1658.62(6) 2 1.747 3.982 860 0.10 × 0.10 × 0.10 2.39 to 27.51 -12,12; -17,17; -18,18 14386 7589 0.0215 6820 99.5% (27.5) 7589/6/407 1.045
Space group Unit cell dimensions: a (A) b (A) c (A)	Pī 9.2814(2) 13.7840(3) 14.0177(2) 83.819(1) 72.394(1) 73.658(1) 1639.79(6) 2 1.743 4.026 848 0.20 × 0.20 × 0.10 2.14 to 27.48 -12,12; -17,17; -18,18 14180 7479 0.0191 6833 99.4% (27.5) 7479/0/389 1.055 0.0239	Pī 11.0420(2) 13.1712(3) 15.4282(3) 83.220(1) 86.225(1) 66.887(1) 2048.82(7) 2 1.667 3.301 1020 0.15 × 0.15 × 0.15 2.06 to 27.50 -14.14; -16,17; -20,20 17381 9226 0.0205 8272 98.0% (27.5) 9226/3/498 1.070 0.0394 0.1046	$P2_1/n$ 13.8657(1) 15.8282(1) 14.9035(1) 90 99.440(2) 90 3226.56(4) 4 1.552 3.848 1504 0.10 × 0.10 × 0.10 2.26 to 27.51 -17.18; -20,19; -19,19 13276 7410 0.0274 5526 99.8% (27.5) 7410/0/389 1.000 0.0298	P1 9.4257(2) 13.8256(3) 13.9046(3) 83.678(1) 71.495(1) 74.952(1) 1658.62(6) 2 1.747 3.982 860 0.10 × 0.10 × 0.10 2.39 to 27.51 -12,12; -17,17; -18,18 14386 7589 0.0215 6820 99.5% (27.5) 7589/6/407 1.045 0.0329 0.0879
Space group Unit cell dimensions: a (A) b (A) c (A)	$P\bar{1}$ 9.2814(2) 13.7840(3) 14.0177(2) 83.819(1) 72.394(1) 73.658(1) 1639.79(6) 2 1.743 4.026 848 0.20 × 0.20 × 0.10 2.14 to 27.48 -12,12; -17,17; -18,18 14180 7479 0.0191 6833 99.4% (27.5) 7479/0/389 1.055 0.0239 0.0560	Pī 11.0420(2) 13.1712(3) 15.4282(3) 83.220(1) 86.225(1) 66.887(1) 2048.82(7) 2 1.667 3.301 1020 0.15 × 0.15 × 0.15 2.06 to 27.50 -14,14; -16,17; -20,20 17381 9226 0.0205 8272 98.0% (27.5) 9226/3/498 1.070 0.0394	$P2_1/n$ 13.8657(1) 15.8282(1) 14.9035(1) 90 99.440(2) 90 3226.56(4) 4 1.552 3.848 1504 0.10 × 0.10 × 0.10 2.26 to 27.51 -17,18; -20,19; -19,19 13276 7410 0.0274 5526 99.8% (27.5) 7410/0/389 1.000 0.0298 0.0602	P1 9.4257(2) 13.8256(3) 13.9046(3) 83.678(1) 71.495(1) 74.952(1) 1658.62(6) 2 1.747 3.982 860 0.10 × 0.10 × 0.10 2.39 to 27.51 -12,12; -17,17; -18,18 14386 7589 0.0215 6820 99.5% (27.5) 7589/6/407 1.045 0.0329

^a Data common to all structures: T = 173(2) K; $\lambda = 0.71073$ Å.

Crystals of $[\mathbf{6d}\text{-H}]^+$ PF_6^- , $[\mathbf{6f}\text{-H}]^+$ PF_6^- , $[\mathbf{6h}\text{-H}]^+$ PF_6^- , and $\mathbf{6f}$, or solvates thereof, were obtained. X-ray data were collected as described above, and refinement afforded the structures in Figs. 3 and 4, and the metrical parameters summarized in Tables 4 and

5. The structures of $[\mathbf{6f}\text{-H}]^+$ $PF_6^- \cdot (CH_2Cl_2)_{1.5}$ and $\mathbf{6f}$, the rhenium moieties of which differ by only a proton, are presented in Fig. 3. One *N*-benzyl group adopts a different conformation, as analyzed further in the discussion section. Hydrogen bonding was again

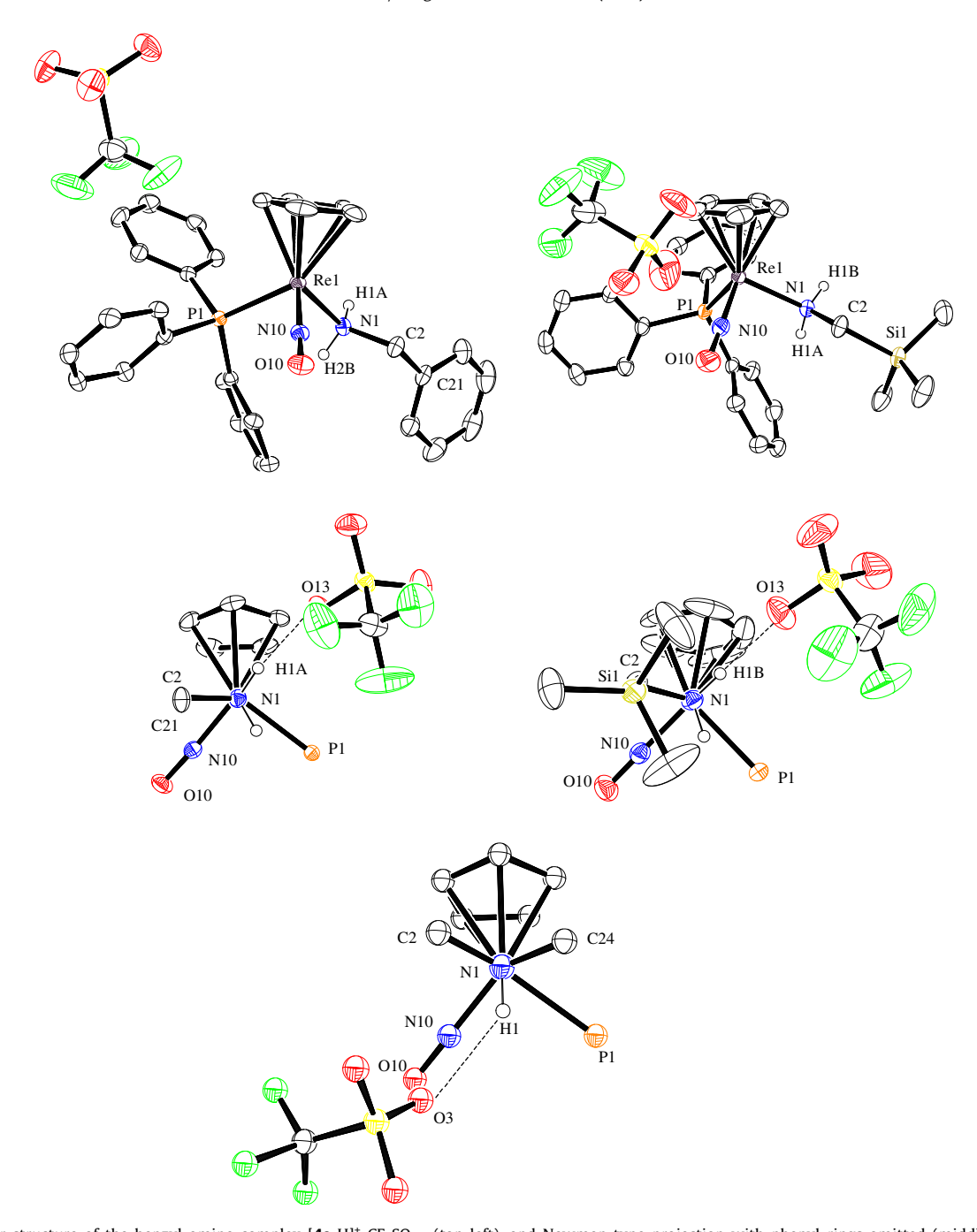


Fig. 1. Molecular structure of the benzyl amine complex [**4a**-H]* CF₃SO₃⁻ (top left), and Newman-type projection with phenyl rings omitted (middle left); molecular structure of the trimethylsilylmethyl amine complex [**4b**-H]* CF₃SO₃⁻ (top right), and Newman-type projection with phenyl rings omitted (middle right); Newman-type interaction of the dimethyl amine complex [**5**-H]* CF₃SO₃⁻ with phenyl rings omitted (bottom). Thermal ellipsoids are rendered at the 50% probability level.

apparent in the salt, but in contrast to $[{\bf 6a'}{\rm -H}]^+$ PF $_6^-$ involved only a single fluorine atom of the anion.

The structures of the closely related diethyl amine adduct [**6d**-H]⁺ $PF_6^- \cdot CH_2Cl_2$ and piperidine adduct [**6h**-H]⁺ $PF_6^- \cdot CH_2Cl_2$ are grouped in Fig. 4. The N1–C4–C5 segment in the former twists relative to that in the latter, as rationalized in the discussion section. As a result, the ethyl group conformations are analogous to those of the N–CH₂–C_{ipso} segments of the benzyl groups of [**6f**-H]⁺ $PF_6^- \cdot (CH_2Cl_2)_{1.5}$. Both salts exhibit hydrogen bonding, but now two fluorine atoms of the hexafluorophosphate anions participate. The exact motif is presumably a function of lattice packing forces.

As shown in Scheme 3 (bottom), the entire sequence with pyrrolidine was repeated starting with the enantiopure rhenium methyl complex $(S)-(\eta^5-C_5H_5)Re(NO)(PPh_3)(CH_3)$. As expected,

this gave the enantiopure salt (S)-[$\mathbf{6g}$ -H]⁺ PF₆⁻ in 82% yield. A subsequent reaction with t-BuOK in THF at room temperature afforded the tertiary amine (S)- $\mathbf{6g}$ in 89% yield. Both complexes were obtained in analytically pure form and exhibited appreciable optical rotations (both dextrorotatory). As in the cases above, retention of configuration at rhenium was presumed.

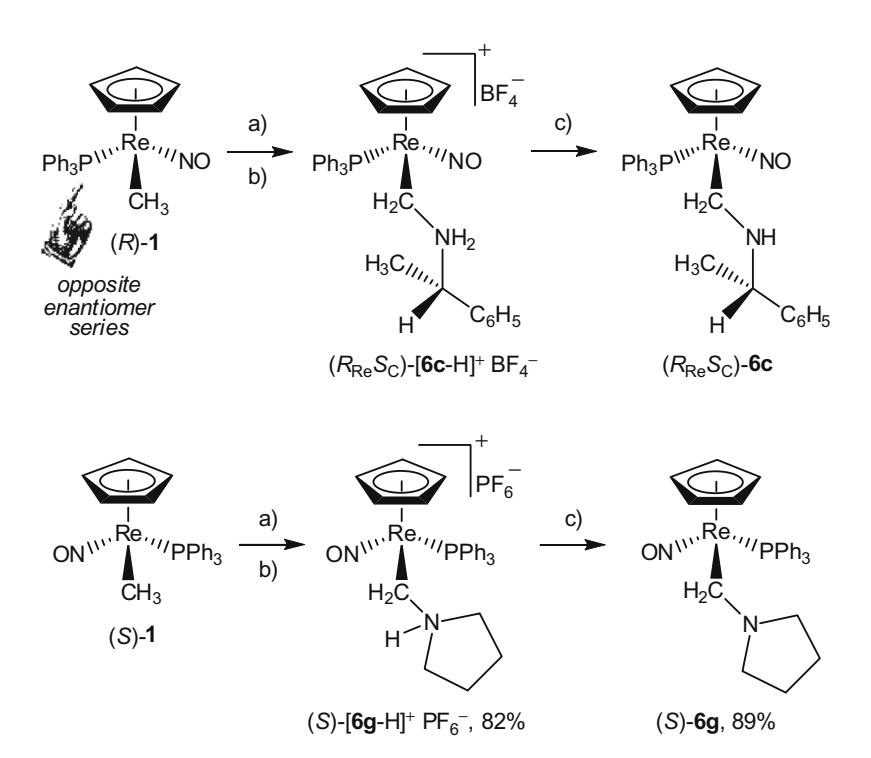
3. Discussion

3.1. Syntheses and stabilities of title complexes

The new rhenium containing amines described above can be divided into three classes: amido complexes ReNRR' (Scheme 1), secondary ReCH₂NHR species (Scheme 2, **6a-c**), and tertiary

Table 2 Key interatomic distances (Å), bond angles (°), and torsion angles (°) for $[\mathbf{4a,b}-H]^+$ $CF_3SO_3^-$ and the previously reported complex $[\mathbf{5}-H]^+$ $CF_3SO_3^-$.

	[4a -H] ⁺ CF ₃ SO ₃ ⁻	[4b -H] ⁺ CF ₃ SO ₃ ⁻ Molecule A	[4b -H] ⁺ CF ₃ SO ₃ ⁻ Molecule B	[5 -H] ⁺ CF ₃ SO ₃ ⁻
Re1-N1	2.169(3)	2.167(3)	2.169(2)	2.193(4)
Re1-P1	2.3548(7)	2.3642(8)	2.3658(8)	2.372(1)
N1-C2	1.494(4)	1.496(4)	1.496(4)	1.478(6)
C2-C21	1.499(4)	1.890(4)	1.896(3)	_
O10-N10	1.195(3)	1.194(4)	1.204(4)	1.176(4)
N10-Re1-N1	96.80(11)	96.07(12)	94.35(11)	92.9(2)
N10-Re1-P1	91.87(8)	88.46(9)	92.16(10)	92.4(1)
N1-Re1-P1	90.24(7)	90.26(7)	89.14(7)	95.4(1)
C2-N1-Re1	114.43(18)	116.0(2)	115.70(19)	112.1(3)
P1-Re1-N1-C2	144.4(2)	148.5(2)	143.9(2)	172.4(7)
N10-Re1-N1-C2	52.5(2)	60.0(3)	51.8(2)	79.7(7)
Re1-N1-C2-C21 or -Si1	179.9(2)	173.67(17)	176.44(15)	-
013···H1A	2.055	1.998	1.953	2.37(6)
013···N1	2.953	2.916	2.864	3.06(5)



Scheme 3. Syntheses of enantiopure rhenium complexes. (a) CH₂Cl₂, Ph₃C⁺ PF₆ or Ph₃C⁺ BF₄ , -78 °C; (b) CH₂Cl₂, (S)-1-phenylethyl amine or pyrrolidine, -78 °C to room temperature; (c) THF, t-BuOK.

ReCH₂NRR' species (Scheme 2, **6d–i**). Each of these can be generated in high yield by standard transformations. However, consistent with earlier studies, the amido complexes are almost always unstable at room temperature [5], although they can usually be isolated as spectroscopically pure powders at low temperatures, and in one case (R/R' = Ph/H) crystallized [5a]. This class of compounds is very unlikely to ever provide a practical catalyst.

In contrast, the tertiary rhenium containing amines $\mathbf{6d-i}$ are robust and are clearly viable candidates for practical catalysts. The secondary amines $\mathbf{6a-c}$ occupy a middle ground. Although samples were quite pure by NMR, none gave a satisfactory microanalysis, and the solids discolorized after several days under nitrogen. These complexes were less stable in solution, but crystals of $(R_{Re}S_C)$ - $\mathbf{6c}$ could nevertheless be obtained.

In this context, there is an obvious relationship between **6a–c** and the α -hydroxyalkyl complex $(\eta^5-C_5H_5)Re(NO)(PPh_3)(CH_2OH)$ [21]. All efforts to isolate or even detect the latter have been unsuc-

cessful. Casey has found that the isolable carbonyl substituted analog $(\eta^5-C_5H_5)Re(NO)(CO)(CH_2OH)$ readily converts to a symmetrical ether with a ReCH₂OCH₂Re linkage [26]. Furthermore, related compounds undergo electrophile induced disproportionations involving initial generation of the methylidene complex $\mathbf{3}^+$ X^- , followed by hydride transfer [21]. However, no well defined rhenium containing decomposition products were noted with $\mathbf{6a}$ – \mathbf{c} .

Despite the lability of **6a-c**, the successful crystallization of $(R_{Re}S_C)$ -**6c** suggests an alternative strategy for resolving racemic chiral at rhenium complexes. Before the convenient method involving the carbonyl complex $[(\eta^5-C_5H_5)Re(NO)(PPh_3)(CO)]^+$ BF₄ was developed [20], the methylidene complex **3**⁺ X⁻ was combined with a number of chiral tertiary amines to give $[ReCH_2NR_3]^+$ species [23] When these were treated with hydride reductants, the methyl complex **1** was regenerated. However, the resulting diastereomers did not prove separable, at least with the chiral amines assayed.

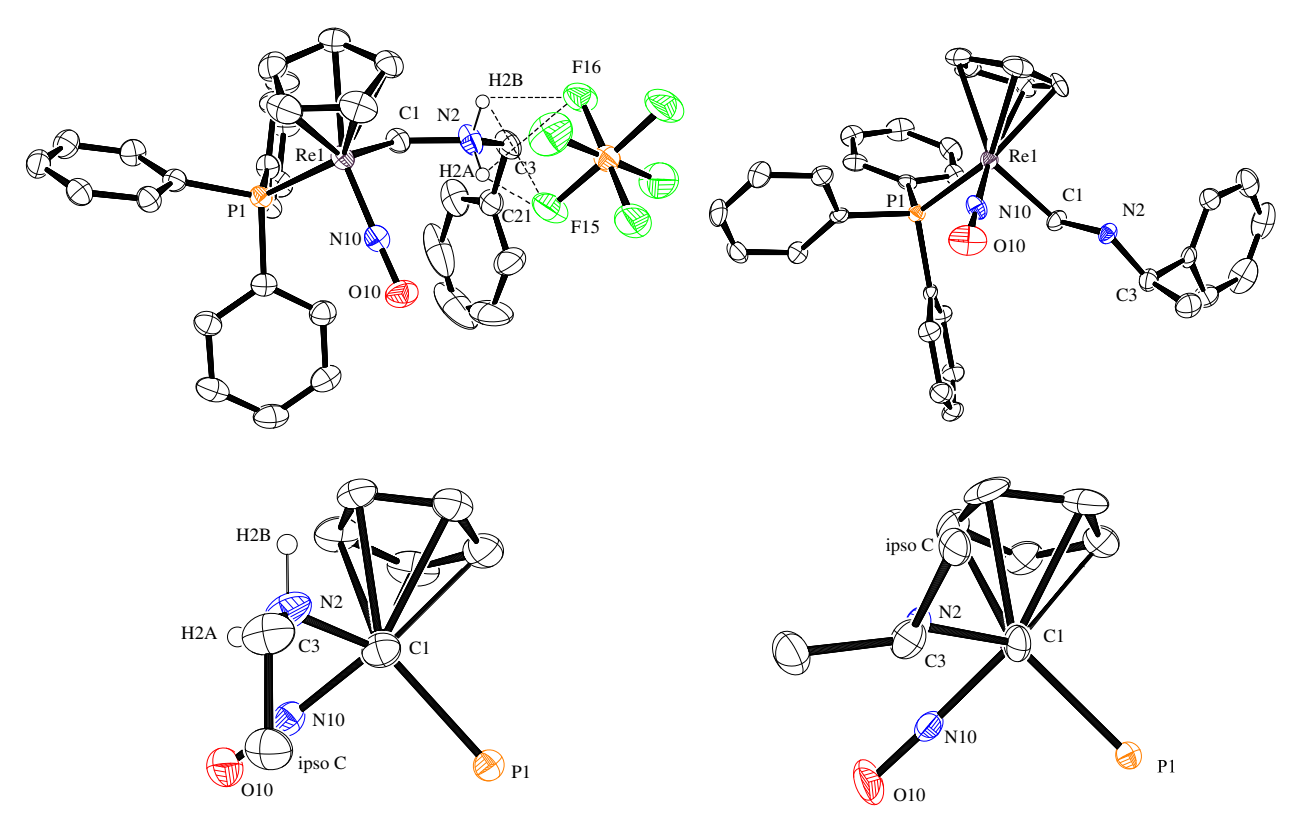


Fig. 2. Molecular structure of $[\mathbf{6a'}-\mathbf{H}]^+$ PF₆ $^-$ (CH₂Cl₂)_{0.5}·(C₆H₆)_{0.5} with solvate molecules omitted (top left), and Newman-type projection with phenyl rings omitted (bottom right). Thermal ellipsoids are rendered at the 50% probability level.

Table 3 Key interatomic distances (Å), bond angles (°), and torsion angles (°) for $[\mathbf{6a'}-H]^*$ $PF_6^- \cdot (CH_2Cl_2)_{0.5} \cdot (C_6H_6)_{0.5}$ and $(R_{Re}S_C)-\mathbf{6c}$.

	$[\mathbf{6a'}\text{-H}]^+ \text{ PF}_6^- \cdot (\text{CH}_2\text{Cl}_2)_{0.5} \cdot (C_6\text{H}_6)_{0.5}$	$(R_{\rm Re}S_{\rm C})$ -6c
Re1-C1 Re1-P1 C1-N2 N2-C3 O10-N10	2.144(4) 2.3827(11) 1.503(5) 1.502(5) 1.203(4)	2.168(9) 2.349(2) 1.479(11) 1.450(11) 1.213(9)
N10-Re1-C1 N10-Re1-P1 C1-Re1-P1 N2-C1-Re1 C3-N2-C1	94.30(15) 93.75(10) 84.67(10) 113.0(2) 115.4(3)	92.9(4) 90.9(3) 88.5(3) 111.7(6) 113.6(7)
P1-Re1-C1-N2 N2-Re1-C1-N1 Re1-C1-N2-C3 C1-N2-C3-C21	155.5(3) 62.1(3) -166.1(3) 58.1(5)	145.7 ^a 54.9 ^a -171.7 ^a -76.1 ^a
F15···H2A F15···H2B F16···H2A F16···H2B F15···N2 F16···N2	2.094 2.965 2.737 2.327 3.896 2.900	- - - - -

^a These values were calculated from the atomic coordinates.

3.2. Structural data

The crystallinity of many of the above complexes has enabled a wealth of new crystal structures that establish new relationships and provide further examples of trends noted previously. As emphasized earlier [27,28], such rhenium complexes are formally octahedral, with the cyclopentadienyl ligand occupying three coordination sites and the remaining ligands defining L–M–L′ bond an-

gles of ca. 90° . Accordingly, the values in Tables 2–5 range from $99.46(17)^{\circ}$ to $84.67(10)^{\circ}$.

As shown in Fig. 1, the benzyl and trimethylsilylmethyl amine complex $[{\bf 4a,b}$ -H] $^+$ CF $_3$ SO $_3$ $^-$ adopt solid state P-Re-N-C conformations with torsion angles of 144.4(2) $^\circ$ and 148.5(2) $^\circ$ -143.9(2) $^\circ$ (Table 2). These place the largest group in the interstice between the small nitrosyl and medium sized cyclopentadienyl ligand, and roughly anti to the bulky PPh $_3$ ligand. Such torsion angles are typical for adducts of the Lewis acid $[(\eta^5-C_5H_5)Re(NO)(PPh_3)]^+$ in which there is a single non-hydrogen substituent on the coordinating atom of the Lewis base. All of the other structures in this paper feature Lewis bases with ReCH $_2$ N linkages, and the analogous torsion angles range from 145.7 $^\circ$ to 177.2(3) $^\circ$.

Similarly, hydrogen bonding in $[4a,b-H]^+$ CF₃SO₃ $^-$ involves the NH protons furthest from the PPh₃ ligands (Fig. 1). Another common feature of $[4a,b-H]^+$ CF₃SO₃ $^-$ concerns the orientations of the CH₂-phenyl and trimethylsilyl groups. The carbon-phenyl and carbon-silicon bonds are essentially anti to the rhenium-nitrogen bonds, as reflected by the Re-N1-C2-C21 (Cipso) and Re-N1-C2-Si torsion angles $(179.9(2)^\circ$ and $173.67(17)^\circ-176.44(15)^\circ$). Past studies have established that the largest group on the atom β to rhenium is normally directed away from the bulky rhenium moiety. The net result is, when viewed from an appropriate perspective, a "W"-like P-Re-X-Y-Z conformation as generalized in III in Fig. 5. This feature is also common to all structures in this paper.

The previously published structure of the dimethyl amine complex $[5-H]^+$ $CF_3SO_3^-$ in Fig. 1 (bottom) illustrates two features. First, when the coordinating atom of the Lewis base possesses *two* non-hydrogen substituents, the torsion angle involving the group anti to the PPh₃ ligand (C2) is often closer to 180° . This directs the other substituent into a less congested region of the PPh₃/cyclopentadienyl interstice. Second, hydrogen bonding

S.N. Seidel et al./Inorganica Chimica Acta 363 (2010) 533-548

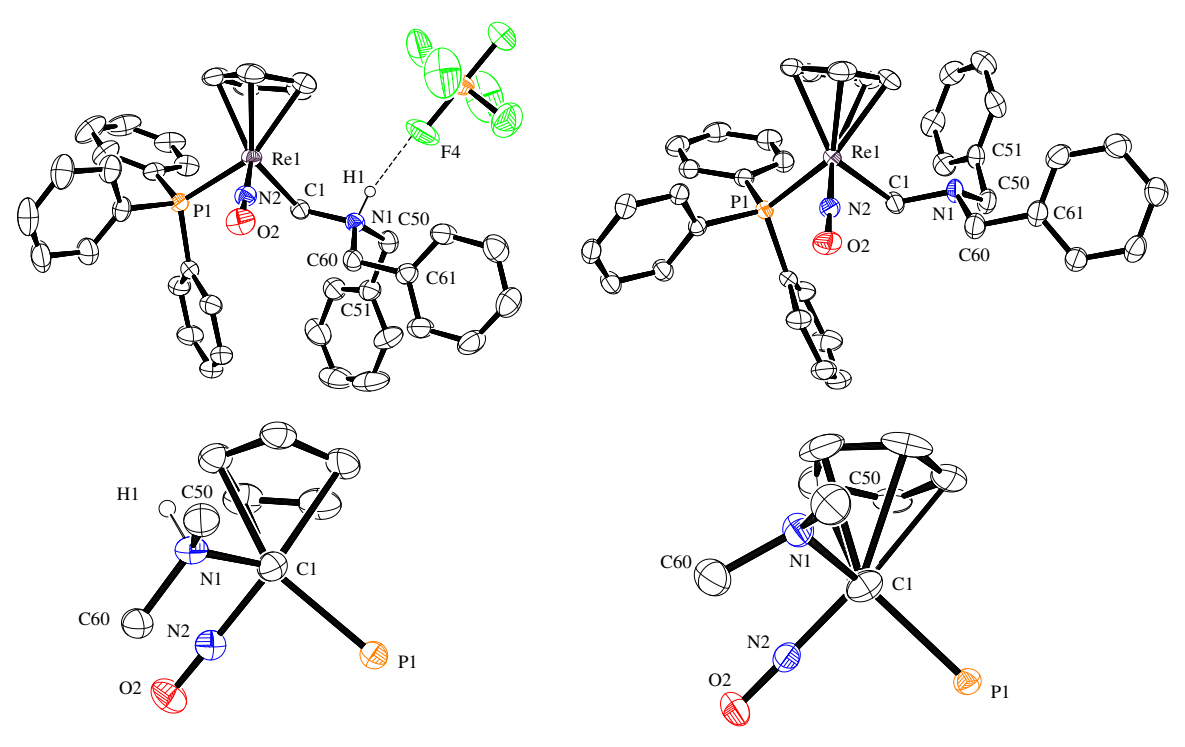


Fig. 3. Molecular structure of $[\mathbf{6f}\text{-H}]^+$ PF $_6^-$ ·(CH₂Cl₂)_{1.5} with solvate molecules omitted (top left), and Newman-type projection of the cation with phenyl rings omitted (bottom left); molecular structure of $\mathbf{6f}$ (top right), and Newman-type projection with phenyl rings omitted (bottom right). Thermal ellipsoids are rendered at the 50% probability level.

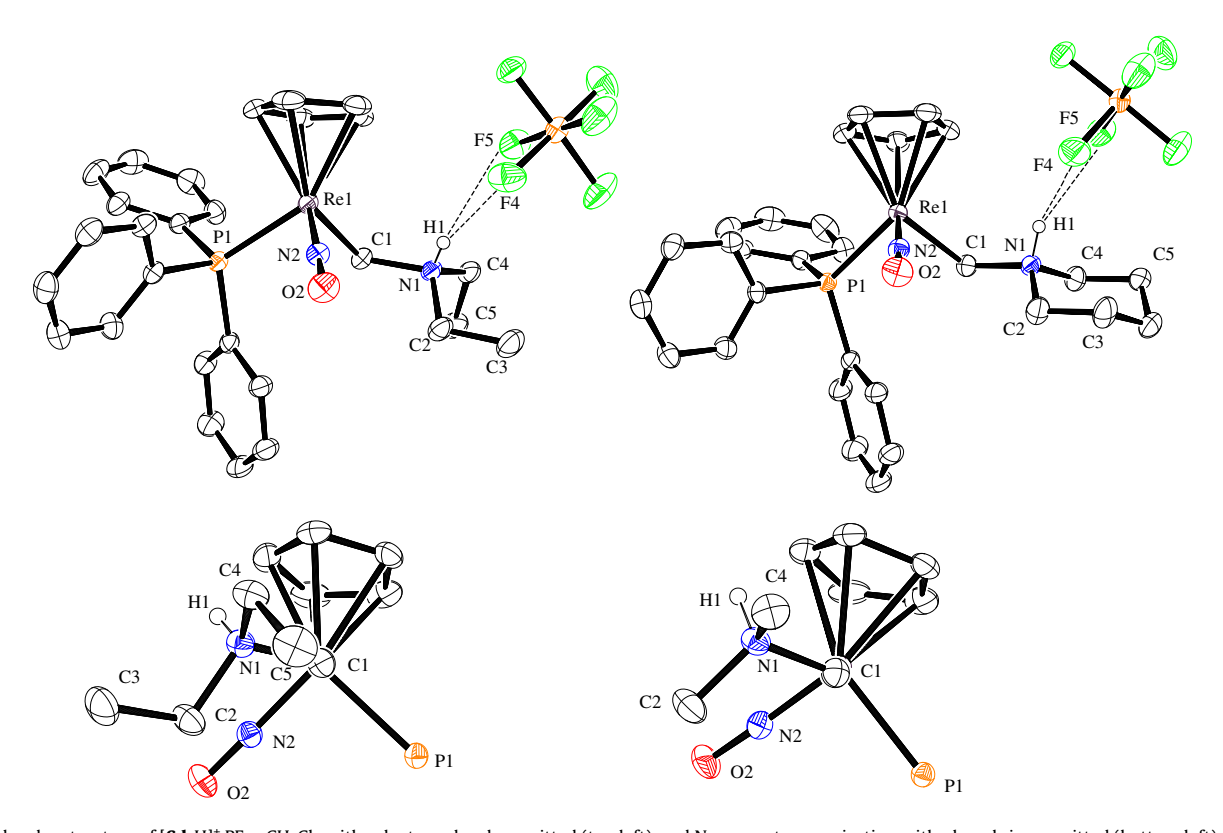


Fig. 4. Molecular structure of $[\mathbf{6d}-\mathbf{H}]^+$ PF₆ $^-$ ·CH₂Cl₂ with solvate molecules omitted (top left), and Newman-type projection with phenyl rings omitted (bottom left); molecular structure of $[\mathbf{6h}-\mathbf{H}]^+$ PF₆ $^-$ ·CH₂Cl₂ with solvate molecules omitted (top right), and Newman-type projection with phenyl rings omitted (bottom right). Thermal ellipsoids are rendered at the 50% probability level.

remains possible when the hydrogen occupies the congested interstice between the large PPh₃ and nitrosyl ligand [27]. Note that the

N-Re-P bond angles are ca. 90°, whereas the P-Re-cyclopentadienyl (centroid) angles are much larger (ca. 135°).

Table 4 Key bond lengths (Å), bond angles (°), and torsion angles (°) for $[\mathbf{6f}\text{-H}]^+$ PF_6^- - $(CH_2Cl_2)_{1.5}$ and $\mathbf{6f}$.

	[6f -H] ⁺ PF ₆ ⁻ ·(CH ₂ Cl ₂) _{1.5}	6f
Re1-C1	2.167(4)	2.175(3)
Re1-P1	2.3570(11)	2.3586(8)
N1-C50	1.519(6)	1.472(5)
N1-C1	1.528(6)	1.475(4)
O2-N2	1.208(5)	1.214(4)
N1-C50	1.519(6)	1.472(5)
N2-Re1-C1	99.46(17)	96.13(13)
N2-Re1-P1	89.17(13)	91.11(9)
C1-Re1-P1	87.24(12)	86.32(9)
C60-N1-C1	110.2(3)	109.4(3)
C50-N1-C1	112.2(3)	109.4(3)
C60-N1-C50	112.9(4)	111.7(3)
N1-C1-Re1	118.0(3)	116.1(2)
P1-Re1-C1-N1	150.6(3)	177.2(3)
N2-Re1-C1-N1	61.9(3)	86.5(3)
C60-N1-C1-Re1	-72.4(4)	-82.8(3)
C1-N1-C50-C51	62.8(5)	-74.0(4)
C1-N1-C60-C61	175.7(4)	175.2(3)
F4···H1	2.042	_
F4···N1	2.884	-

Table 5 Key interatomic distances (Å), bond angles (°), and torsion angles (°) for $[6d-H]^*$ $PF_6^- \cdot CH_2Cl_2$ and $[6h-H]^*$ $PF_6^- \cdot CH_2Cl_2$.

	[6d -H] ⁺ PF ₆ ⁻ -CH ₂ Cl ₂	$[\mathbf{6h}\text{-H}]^+ \text{PF}_6^- \cdot \text{CH}_2 \text{Cl}_2$
Re1-C1	2.162(3)	2.162(4)
Re1-P1	2.3514(7)	2.3547(10)
N1-C1	1.529(3)	1.532(5)
N1-C4	1.515(3)	1.490(5)
02-N2	1.206(3)	1.211(5)
N2-Re1-C1	98.67(11)	99.13(15)
N2-Re1-P1	91.32(8)	92.06(11)
C1-Re1-P1	87.62(8)	87.56(11)
N1-C1-Re1	116.48(18)	116.8(3)
C2-N1-C1	110.9(2)	111.1(3)
C2-N1-C4	113.4(2)	110.2(3)
C4-N1-C1	112.5(2)	110.9(3)
P1-Re1-C1-N1	-149.88(18)	-151.2(3)
N2-Re1-C1-N1	-58.9(2)	-59.6(3)
C2-N1-C1-Re1	84.8(2)	81.6(4)
C4-N1-C2-C3	54.9(4)	56.0(5)
C1-N1-C2-C3	-177.3(3)	-179.5(3)
C1-N1-C4-C5	-66.5(3)	179.4(4)
C2-N1-C4-C5	60.5(3)	-56.0(5)
F4···H1	2.338	2.265
F5···H1	2.671	2.589
F4···N2	3.074	3.144
F5···N2	3.227	3.350

Fig. 2 presents two molecules, $[\mathbf{6a'}\text{-H}]^+$ PF₆ $^-$ and $(R_{Re}S_C)$ - $\mathbf{6c}$ or solvates thereof, which formally differ by a H/CH₃ substitution and the addition of HPF₆. The P–Re–C1–N2 torsion angles are quite similar (Table 3; 155.3(3)° versus 145.7°). Also, the Re–C1–N2–C3 torsion angles are near $\pm 180^\circ$ ($-166.1(3)^\circ$, -171.7°), directing the *N*-alkyl group away from the bulky rhenium moiety. However, the conformations about the N2–C3 bonds differ, as evidenced by the C1–N2–C3–C_{ipso} torsion angles (58.1(5)°, -76.1°). Thus, the phenyl groups occupy different positions.

Fig. 3 depicts the structures of **6f** and its HPF₆ adduct, [**6f**-H][†] PF₆⁻, both of which feature a dibenzylamino moiety. The Newman projections show that the rhenium-carbon conformations vary slightly, as quantified by a ca. 26° difference in the P1–Re–C2–N1 torsion angles (Table 4). The pro-R benzyl groups (which contain C60 and C61) adopt similar conformations about the N–CH₂ link-

ages. However, the pro-S benzyl groups (C50, C51) do not, as reflected by a ca. 136° difference in the C1–N1–C50–C51 torsion angles. As a consequence, the C50–C51 linkage in [**6f**-H] $^+$ PF $_6$ $^-$ is gauche to both the C1–N1 and C60–N1 moieties, rendering the NH group more accessible for hydrogen bonding. Otherwise, the structures are quite similar. In **6f**, the sum of the bond angles about N1 is 330.5°, indicative of a strongly pyramidalized nitrogen atom (limiting values for ideal tetrahedral and planar geometries, 328.5° and 360°). The sum of the C–N–C bond angles in [**6f**-H] $^+$ PF $_6$ $^-$ (335.3°) is slightly higher.

Fig. 4 depicts the structures of two related salts, the diethyl amine and piperidine adducts [**6d,h**-H] $^+$ PF $_6^-$. These differ by the single carbon atom needed to connect the methyl groups of [**6d**-H] $^+$ PF $_6^-$, and crystallize in the same space group and with very similar lattice constants (Table 1). The only significant difference involves the N1–C4–C5 linkage or pro-S ethyl group of [**6d**-H] $^+$ PF $_6^-$, which unlike the corresponding unit in [**6h**-H] $^+$ PF $_6^-$ is not constrained in a ring. Accordingly, the C5 methyl group twists to avoid an unfavorable non-bonding 1,5-syn-pentane-type interaction [29] with the C3 methyl group. As a result, the C4–C5 linkage of [**6d**-H] $^+$ PF $_6^-$ is gauche to both the C1–N1 and C2–N1 moieties, analogous to the situation for the pro-S benzyl group in [**6f**-H] $^+$ PF $_6^-$. The sums of the C–N–C bond angles about N1 in [**6d,h**-H] $^+$ PF $_6^-$ are 336.8° and 332.2°, respectively.

By coincidence, all of the chiral at rhenium complexes in this paper with an S absolute configuration have the same relative configuration. Thus, it is a simple matter to compare the propeller chiralities of the PPh₃ ligands [30] in the crystallographically characterized species. Interestingly with the exception of $[\mathbf{6a'}\text{-H}]^+$ PF₆ $^-$ (CH₂Cl₂)_{0.5}·(C₆H₆)_{0.5}, all complexes exhibit the same relative propeller configurations. In no case are any phenyl/phenyl stacking interactions evident. Such propeller diastereomers of course rapidly interconvert in solution. Similar biases involving propeller configurations have been noted in other series of chiral rhenium complexes [29].

There are numerous special applications for sterically encumbered bases in organic synthesis. In the course of analyzing the above structures, it was noted that the nitrogen atoms are very shielded. A representative structure with all atoms at van der Waals radii ($\bf{6f}$) is depicted in Fig. 5. In earlier studies, it was shown that amido complexes (η^5 -C₅H₅)Re(NO)(PPh₃)(NHR) may be lithiated to give (η^5 -C₅H₅)Re(NO)(PPh₃)(NLiR) species [5b]. This suggests the possibility of accessing what might be termed a "chiral organometallic LDA". Unfortunately, the lithiated complexes were too unstable for practical use in synthesis. However, related species derived from $\bf{6a}$ - \bf{c} remain to be investigated.

3.3. Exploratory chemistry

As described elsewhere, complexes **6d-i** have been screened as catalysts for a number of enantioselective transformations that are known to be effected by chiral organic amines [17]. In all cases, results have been disappointing. Either no reactions were observed, or the products were racemic (and the rates modest). Certain reactions are best catalyzed by bifunctional amines, and for this reason the alcohol containing base **6i** was also investigated. This complex can be compared to the monorhenium species derived from *N*,*N*′-diethylethylene diamine in Chart 1 (bottom right) [11], which represents another type of bifunctional amine. Since the rhenium substituted terminus of the diamine is more basic, the ammonium proton is localized on the ReCH₂N moiety.

The salt $(R_{\text{Re}}S_{\text{C}})$ –[**6c**-H]⁺ BF₄⁻ was also used as a lead compound in a study of enantioselective protonations [31,32]. Naproxen derivatives could be obtained in up to 30% ee, but the methodology was not competitive with other protocols. In another thrust, attempts were made to oxidize the pyrrolidine derived species **6g**

S.N. Seidel et al./Inorganica Chimica Acta 363 (2010) 533-548

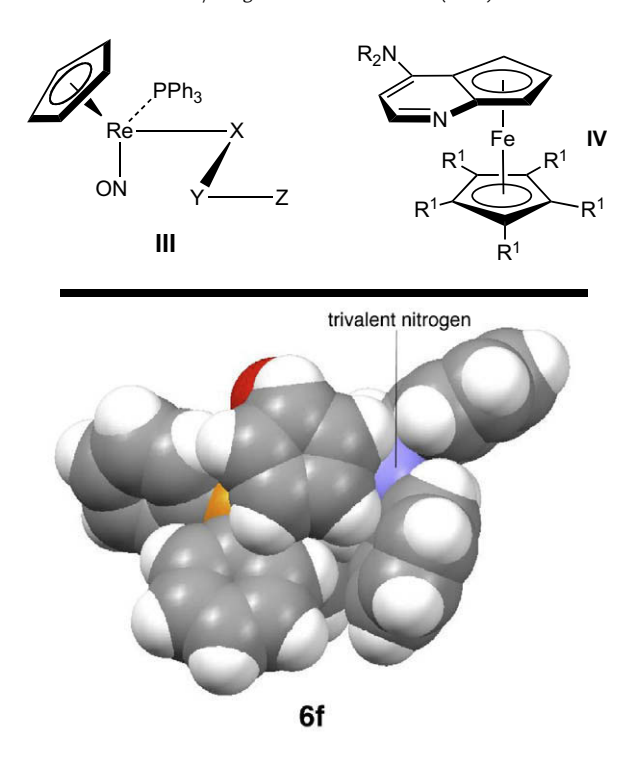


Fig. 5. Additional structural perspectives and catalysts: "W" like conformation common to all structures (upper left); a class of chiral iron containing amines that have been extensively exploited by Fu in enantioselective catalysis (upper right); a space filling model of **6f**, illustrating the steric congestion about the dibenzyl amino moiety.

to an *N*-oxide [33]. A number of common oxidants (PhIO, dimethyl dioxirane, *m*-CPBA, Me₃SiOOSiMe₃/MeReO₃) have given reasonably clean reactions, but it has not yet proved possible to purify a product. Finally, it should be noted that Fu has successfully applied a series of ferrocene-derived chiral amines (**IV**, Fig. 5) in a number of enantioselective reactions [34]. In these systems, the nitrogen atom is part of a pyridinyl system.

While this study was in progress, it was found that analogous ReCH₂PRR' species are excellent enantioselective catalysts for a variety of phosphine-catalyzed transformations [16]. Given the disappointing results with **6d-i** in similar processes, this study was truncated at the above stage. Nonetheless, this work has established the ready availability of a variety rhenium containing tertiary amines with ReCH₂NRR' linkages, as well as their somewhat less stable secondary ReCH₂NHR counterparts. Also, other types of rhenium containing amines may prove to be more effective in catalysis, and efforts with quinoline and isoquinoline species are in progress and will be reported in due course [35].

4. Experimental

4.1. General data

All reactions were conducted under nitrogen. NMR spectra were recorded on Bruker Avance spectrometers (300 or 400 MHz) at 25–28 °C and referenced to the residual solvent signal (1 H: $C_{6}D_{5}$ H, 7.15 ppm; CDHCl₂, 5.32 ppm; CD₂HCN, 1.93 ppm; $^{13}C_{1}^{1}H$ }: $C_{6}D_{6}$, 128.0 ppm; CD₂Cl₂, 53.5 ppm; CD₃CN, 1.30 ppm). IR spectra were recorded on an ASI React IR®-1000 spectrometer. Mass spectra were obtained using a Micromass Zabspec instrument. Elemental analyses were determined with a Carlo Erba EA1110 CHN instrument. Optical rotations were determined as described previously [36] using a Perkin–Elmer model 341 polarimeter.

Solvents were treated as follows: CH₂Cl₂ (Staub), distilled from CaH₂; benzene, toluene, diethyl ether, THF, and *n*-pentane

 $(5 \times Gr\ddot{u}ssing)$, distilled from sodium/benzophenone; ethanol and hexanes $(2 \times Staub)$, distilled without additional treatment; CD₃CN, CDCl₃, CD₂Cl₂, and C₆D₆ (4 × Deutero GmbH), used as received.

Chemicals were treated as follows: Ph_3C^+ PF_6^- (>95.0%, Fluka) and Ph_3C^+ BF_4^- (>98%, Fluka) were stored under argon in a glove box at -32 °C; [37] CF_3SO_3H (Acros, 99%), n-butyl amine (Acros, 99.8%), benzyl amine (Acros, 99.5+%), (S)-1-phenylethyl amine (Lancaster, 98%), diethyl amine (Acros, 99%), di-n-butyl amine (Acros, 99.5%), dibenzyl amine (Acros, 98%), piperidine (Aldrich, >99.5%), pyrrolidine (Acros, 99+%), methyl 2-hydroxyethyl amine (Acros, 99+%), t-BuOK (Acros, 98+%, or Aldrich, 1.0 M in THF), and Celite® 535 (Merck) were used as received.

4.1.1. $[(\eta^5 - C_5H_5)Re(NO)(PPh_3)(NH_2CH_2C_6H_5)]^+ CF_3SO_3^- ([\textbf{4a}-H]^+ CF_3SO_3^-)$

A Schlenk flask was charged with $(\eta^5-C_5H_5)Re(NO)(PPh_3)(CH_3)$ (1; [20] 0.104 g, 0.186 mmol) and CH_2Cl_2 (5 mL), and cooled to 0 °C. Then CF_3SO_3H (0.027 mL, 0.048 g, 0.32 mmol) was added with stirring. After 1 h, benzyl amine (0.061 mL, 0.060 g, 0.56 mmol) was added. After 30 min, the sample was concentrated by oil pump vacuum (to ca. 2 mL). Then hexanes (7 mL) were rapidly added and a yellow powder precipitated, which was collected by filtration, washed with hexanes (2 × 4 mL), and dried by oil pump vacuum to give [4a-H]* CF_3SO_3 (0.0520 g, 0.0650 mmol, 73%). M.p. 165–167 °C (capillary). Elemental Anal. Calc. for $C_{31}H_{29}F_3N_2O_4PReS$ (799.8): C, 46.55; H, 3.65; N, 3.50; S, 4.01. Found: C, 46.19; H, 3.46; N, 3.40; S, 4.13%.

NMR (CD₂Cl₂, δ in ppm). 1 H (400 MHz): 7.69–7.38 (m, 4 C₆ H_5 , 8H), 7.17–6.96 (m, 4 C₆ H_5 , 12H), 5.92 (br s, NHH', 1H), 5.39 (s, C₅ H_5 , 5H), 4.08–4.01 (m, NH₂CH₂ and NHH', 3H); 13 C{ 1 H} (101 MHz): PPh₃ at 133.9 (d, 2 J(C,P) = 10.9 Hz, o), 132.0 (s, p), 131.9 (d, 1 J(C,P) = 55.0 Hz, *i*), 129.8 (d, 3 J(C,P) = 10.8 Hz, *m*); 137.4, 129.5, 129.3, 129.1 (4 s, CH₂C₆H₅), 120.9 (q, 1 J(C,F) = 320 Hz, CF₃), 91.7 (s, C₅H₅), 61.6 (s, NCH₂); 31 P{ 1 H} (162 MHz): 21.3 (s, PPh₃); 19 F{ 1 H} (282 MHz): $^{-79.2}$ (s, CF₃SO₃).

IR: 1 1687 (ν_{NO} , s). MS: 2a 651 (100) [**4a**] $^+$, 544 (55) [**4a**-NHCH₂C₆H₅] $^+$.

4.1.2. $(\eta^5 - C_5H_5)Re(NO)(PPh_3)(NHCH_2C_6H_5)$ (**4a**)

A Schlenk flask was charged with $[4a-H]^+$ CF₃SO₃⁻ (0.0700 g, 0.0875 mmol) and THF (5 mL). Then t-BuOK (0.0110 g, 0.0875 mmol) was added with stirring. After 30 min, the solvent was removed from the nearly homogeneous mixture by oil pump vacuum. Benzene (6 mL) was added, and the sample was filtered through a glass frit. The solvent was removed from the filtrate by oil pump vacuum to give 4a as an orange powder (0.0430 g, 0.0661 mmol, 76%) of ca. 95% purity (31 P NMR). Due to the labile nature of this compound, it was characterized only by NMR (1 H, 31 P{ 1 H}).

NMR (C_6D_6 , δ in ppm). 1 H (400 MHz): 7.49–7.47 (m, 4 C_6H_5 , 8H), 7.24–7.19 (m, 4 C_6H_5 , 2H), 7.01–6.96 (m, 4 C_6H_5 , 10H), 5.14 (s, C_5H_5 , 5H), 4.77 (br s, NH₂CH₂, 2H); 31 P{ 1 H} (162 MHz): 29.4 (s, PPh_3).

4.1.3. $[(\eta^5 - C_5H_5)Re(NO)(PPh_3)(CH_2NH_2CH_2C_6H_5)]^+$ BF₄⁻ ([**6a**-H]⁺ BF₄⁻)

A Schlenk flask was charged with **1** (0.226 g, 0.405 mmol) [20] and CH_2Cl_2 (10 mL), and cooled to -78 °C. Then Ph_3C^+ BF_4^- (0.176 g, 0.486 mmol) was added with stirring. After 30 min, benzyl amine (0.017 mL, 0.017 g, 0.16 mmol) was added. After 20 min, the cold bath was removed. After 30 min, the sample was concentrated by oil pump vacuum (to ca. 3 mL). Diethyl ether (7 mL) was added. A yellow powder precipitated, which was collected by filtration, washed with diethyl ether (2 × 3 mL), and dried by oil pump vacuum to give [**6a**-H]⁺ BF_4^- (CH_2Cl_2)_{0.5} (0.198 g, 0.249 mmol, 62%)³. M.p. 174–177 °C (capillary). Elemental Anal. Calc. for $C_{31}H_{31}BF_4N_2OPRe\cdot(CH_2Cl_2)_{0.5}$ (794): C, 47.65; H, 4.06; N, 3.53. Found: C, 47.44; H, 4.07; N, 3.52%.

NMR (CD₂Cl₂, δ in ppm). ¹H (400 MHz): 7.49–7.42 (m, 4 C₆H₅, 12H), 7.28–7.19 (m, 4 C₆H₅, 8H), 6.80 (br s, NHH', 1H), 5.29 (br s, NHH', 1H), 5.22 (s, C₅H₅, 5H), 4.08–3.99 (m, ReCHH', 1H), 3.49–3.46 (m, ReCHH' and NH₂CH₂C₆H₅, 3H); ¹³C{¹H} (101 MHz): PPh₃ at 134.5 (d, ¹J(C,P) = 54.3 Hz, *i*), 133.6 (d, ²J(C,P) = 10.0 Hz, *o*), 131.6 (s, *p*), 129.2 (d, ³J(C,P) = 10.0 Hz, *m*); 131.1, 130.1, 129.7, 129.6 (4 s, CH₂C₆H₅), 90.9 (s, C₅H₅), 56.0 (s, CH₂C₆H₅), 18.7 (s, ReCH₂); ³¹P{¹H} (162 MHz): 22.1 (s, PPh₃).

IR: 1 1640 (ν_{NO} , s). MS: 2b 664 (9) [**6a**-H] $^{+}$, 559 (100) [**6a**-CH₂NH₂CH₂C₆H₅] $^{+}$.

4.1.4. $[(\eta^5 - C_5H_5)Re(NO)(PPh_3)(CH_2NH_2CH_2C_6H_5)]^+$ PF $_6^-$ ([$\boldsymbol{6a}' - H$] $^+$ PF $_6^-$)

Complex **1** (0.0803 g, 0.143 mmol), [20] CH_2Cl_2 (10 mL), Ph_3C^+ PF_6^- (0.0583 g, 0.150 mmol), and benzyl amine (0.016 mL, 0.015 g, 0.14 mmol) were combined in a procedure analogous to that for [**6a**-H]* BF_4^- . In a similar workup, the sample was concentrated by oil pump vacuum (to ca. 5 mL). Then n-pentane (7 mL) was added. A yellow powder precipitated, which was collected by filtration, washed with n-pentane (2 × 3 mL), and dried by oil pump vacuum to give [**6a**'-H]* PF_6^- (0.111 g, 0.137 mmol, 96%)³. M.p. $166-169\,^{\circ}\text{C}$ (capillary). Elemental Anal. Calc. for $\text{C}_{31}\text{H}_{31}\text{F}_6\text{N}_2\text{OP}_2\text{Re}$ (810.6): C, 45.98; H, 3.86; N, 4.46. Found: C, 45.60; H, 3.98; N, 3.45%.

NMR (CD₂Cl₂, δ in ppm). ¹H (400 MHz): 7.42–7.33 (m, 4 C₆H₅, 12H), 7.21–7.20 (m, 4 C₆H₅, 8H), 6.03 (br s, NHH', 1H), 5.45 (br s, NHH', 1H), 5.19 (s, C₅H₅, 5H), 4.18–4.15 (m, ReCHH', 1H), 4.06–

3.97 (m, ReCHH' and C H_2 C₆H₅, 3H); ¹³C{¹H} (101 MHz): PPh₃ at 134.3 (d, 1J (C,P) = 54.1 Hz, i), 133.6 (d, 2J (C,P) = 10.8 Hz, o), 131.1 (d, 4J (C,P) = 6.5 Hz, p), 129.2 (d, 3J (C,P) = 10.4 Hz, m); 130.1, 129.9, 129.7, 128.6 (4 s, CH₂C₆H₅), 91.0 (s, C₅H₅), 56.5 (s, NCH₂), 19.1 (s, ReCH₂); ³¹P{¹H} (162 MHz): 21.3 (s, PPh₃), -143.9 (sep, 1J (P,F) = 712 Hz, PF₆).

IR: 1 1644 (v_{NO} , s). MS: 2a 663 (26) [**6a**'-H]⁺, 558 (100) [**6a**'-NH₂CH₂C₆H₅)]⁺.

4.1.5. $(\eta^5 - C_5H_5)Re(NO)(PPh_3)(CH_2NHCH_2C_6H_5)$ (**6a**)

A Schlenk flask was charged with $[6a'-H]^+$ PF₆ $^-$ (0.101 g, 0.135 mmol) and THF (5 mL). Then t-BuOK (0.0228 g, 0.203 mmol) was added with stirring. After 2 h, the solvent was removed from the nearly homogeneous mixture by oil pump vacuum. Benzene (7 mL) was added, and the sample was filtered through a Celite plug. The solvent was removed from the filtrate by oil pump vacuum to give 6a as an orange powder (0.0672 g, 0.0993 mmol, 74%) of ca. 95% purity (31 P NMR).

NMR (C_6D_6 , δ in ppm). ¹H (400 MHz): 7.45–7.41 (m, 4 C_6H_5 , 10H), 7.22–7.19 (m, 4 C_6H_5 , 6H), 7.04–6.98 (m, 4 C_6H_5 , 9H), 4.67 (s, C_5H_5 , 5H), 4.27–4.22 (m, ReCHH′, 1H), 4.07–4.03, 3.95–3.93 (2 m, NH₂CHH′C₆H₅, 2 × 1H), 3.87–3.82 (m, ReCHH′, 1H); ¹³C{¹H} (76 MHz): PPh₃ at 137.5 (d, ¹J(C,P) = 51.7 Hz, *i*), 134.2 (d, ²J(C,P) = 10.8 Hz, *o*), 130.2 (d, ⁴J(C,P) = 2.2 Hz, *p*), 129.0 (s (other line of expected d obscured), *m*); 128.8, 127.9, 126.8 (3 s, CH₂C₆H₅), 90.3 (s, C_5H_5), 59.5 (s, NCH₂), 20.4 (s, ReCH₂); ³¹P{¹H} (162 MHz): 25.0 (s, PPh₃), –4.0 (s, free PPh₃).⁴

IR: 1 1617 (v_{NO} , s). MS: 2a 664 (55) [**6a**]⁺, 558 (100) [**6a**-NH₂CH₂C₆H₅)]⁺.

4.1.6. $[(\eta^5 - C_5H_5)Re(NO)(PPh_3)(CH_2NH_2CH_2CH_2CH_2CH_3)]^+ PF_6^- ([\mathbf{6b}-H]^+ PF_c^-)$

Complex **1** (0.124 g, 0.222 mmol), [20] CH_2Cl_2 (6 mL), Ph_3C^+ PF_6^- (0.0947 g, 0.244 mmol), and n-butyl amine (0.024 mL, 0.018 g, 0.24 mmol) were combined in a procedure analogous to that for [**6a**′-H]⁺ PF_6^- . A similar workup (sample concentration to ca. 5 mL; addition of 6 mL of n-pentane) gave [**6b**-H]⁺ PF_6^- . (CH_2Cl_2)_{0.33} (0.174 g, 0.216 mmol, 97%) as a yellow powder. M.p. 178–180 °C (capillary). Elemental Anal. Calc. for $\text{C}_2\text{B}\text{H}_3\text{F}_6\text{N}_2\text{O}\text{-P}_2\text{Re}$ ·(CH₂Cl₂)_{0.33} (803.3): C, 42.32; H, 4.22; N, 3.48. Found: C, 42.56; H, 4.33; N, 3.57%.

NMR (CD₂Cl₂, δ in ppm). 1 H (400 MHz): 7.61–7.41 (m, 3 C₆H₅, 9H), 7.32–7.28 (m, 3 C₆H₅, 6H), 5.80 (br s, NHH', 1H), 5.24 (s, C₅H₅, 5H), 4.98 (br s, NHH', 1H), 4.14–4.10 (m, ReCHH', 1H), 3.99–3.89 (m, ReCHH', 1H), 2.95–2.90 (m, NH₂CH₂, 2H), 1.52–1.49 (m, NH₂CH₂CH₂, 2H), 1.36–1.29 (m, NH₂CH₂CH₂CH₂, 2H), 0.91 (t, 3 J(H,H) = 5.1 Hz, CH₃, 3H); 13 C{ 1 H} (101 MHz): PPh₃ at 134.5 (d, 1 J(C,P) = 54.0 Hz, *i*), 133.7 (d, 2 J(C,P) = 10.6 Hz, *o*), 131.2 (s, *p*), 129.2 (d, 3 J(C,P) = 10.7 Hz, *m*); 90.9 (s, C₅H₅), 52.6 (s, NCH₂), 27.9 (s, ReCH₂), 19.9 (s, NCH₂CH₂), 19.7 (s, NCH₂CH₂CH₂), 13.6 (s, CH₃); 31 P{ 1 H} (162 MHz): 21.9 (s, PPh₃), –144.0 (sep, 1 J(P,F) = 712 Hz, PF₆).

IR:¹ 1633 (ν_{NO} , s). MS:^{2a} 629 (20) [**6b**-H]⁺, 558 (100) [**6b**-NH₂CH₂CH₂CH₂CH₃]⁺.

4.1.7. $(\eta^5 - C_5H_5)Re(NO)(PPh_3)(CH_2NHCH_2CH_2CH_2CH_3)$ (**6b**)

The salt [$\mathbf{6b}$ -H]⁺ PF₆⁻ (0.132 g, 0.170 mmol), THF (7 mL), and t-BuOK (0.0287 g, 0.256 mmol) were combined in a procedure analogous to that for $\mathbf{6a}$. An identical workup gave $\mathbf{6b}$ as an orange powder (0.0885 g, 0.141 mmol, 83%) of ca. 99% purity (31 P NMR).

NMR (C_6D_6 , δ in ppm). ¹H (400 MHz): 7.55–7.51 (m, 3 C_6H_5 , 6H), 7.05–6.98 (m, 3 C_6H_5 , 9H), 4.77 (s, C_5H_5 , 5H), 4.25 (d, C_5H_5) = 10.4 Hz, ReCHH', 1H), 3.97 (d, C_5H_5) = 10.4 Hz, ReCHH',

¹ Powder film, cm⁻¹.

 $^{^2\,}$ m/z (%); the peaks correspond to the most intense signal of the isotope envelope: (a) FAB, 3-NBA. (b) MALDI TOF, DCTB.

³ With some batches, recrystallization from CH₂ Cl₂/n-pentane was required to remove byproducts.

⁴ The amount of PPh₃ increases with time.

1H), 2.90–2.87 (m, NH₂CHH', 1H), 2.71–2.66 (m, NH₂CHH', 1H), 1.58–1.32 (m, NH₂CH₂CH₂CH₂, 4H), 0.91 (t, ${}^{3}J(H,H) = 7.2$ Hz, CH₃, 3H); ${}^{13}C\{{}^{1}H\}$ (101 MHz): PPh₃ at 137.5 (d, ${}^{1}J(C,P) = 51.4$ Hz, i), 134.1 (d, ${}^{2}J(C,P) = 10.4$ Hz, o), 130.2 (s, p), 128.6 (d, ${}^{3}J(C,P) = 10.2$ Hz, m); 90.2 (s, $C_{5}H_{5}$), 55.6 (s, NCH₂), 33.9 (s, NCH₂CH₂), 21.4 (s, NCH₂CH₂CH₂), 20.4 (s, ReCH₂), 14.7 (s, CH₃); ${}^{31}P\{{}^{1}H\}$ (162 MHz): 26.6 (s, PPh₃).

IR:¹ 1614 (ν_{NO} , s). MS:^{2a} 629 (46) [**6b**]⁺, 558 (100) [**6b**-NHCH₂CH₂CH₂CH₃]⁺.

4.1.8. $(S_{Re}S_C)/(R_{Re}S_C)-[(C_5H_5)Re(NO)(PPh_3)(CH_2NH_2CH(CH_3)(C_6H_5))]^+$ BF₄ $^ ([\textbf{6c}-H]^+$ BF₄ $^-$)

Complex **1** (0.200 g, 0.358 mmol), [20] CH_2Cl_2 (8 mL), Ph_3C^+ BF_4^- (0.130 g, 0.394 mmol), and (*S*)-1-phenylethyl amine (0.050 mL, 0.048 g, 0.39 mmol) were combined in a procedure analogous to that for [**6a**'-H]⁺ PF_6^- . A similar workup (sample concentration to ca. 5 mL; addition of 7 mL of *n*-pentane) gave [**6c**-H]⁺ BF_4^- (0.264 g, 0.345 mmol, 97%; 48:52 diastereomer mixture) as a yellow powder.³ M.p. 141–142 °C, dec (capillary). Elemental Anal. Calc. for $C_{32}H_{33}BF_4N_2OPRe$ (765.6): C, 50.20; H, 4.34; N, 3.66. Found: C, 49.92; H, 4.18; N, 3.46%.

NMR (CD₂Cl₂, δ in ppm). 1 H (300 MHz): 7.90–7.30 (m, 4 C₆H₅, 20H), 6.47, 6.11 (2 br s, NHH′ and NHH′, 2 × 1H), 5.39/5.32 (2 s, C₅H₅, 5H, 48:52), 4.45–4.23 (m, CHCH₃, 1H), 4.06–4.01 (m, ReCHH′, 1H), 3.94–3.90 (m, ReCHH′, 1H), 1.80/1.73 (2 d, 3 J(H,H) = 6.9/6.6 Hz, CH₃, 3H, 48:52); 13 C{ 1 H} (76 MHz): PPh₃ at 134.5/134.4 (2 d, 1 J(C,P) = 53.2/53.6 Hz, i), 133.5/133.4 (2 d, 2 J(C,P) = 10.6/10.5 Hz, o), 131.1/131.0 (2 s, p), 129.1/129.0 (2 d, 3 J(C,P) = 10.4/10.4 Hz, m); 137.1/136.4 (2 s, CHi-C₆H₅), 129.8/129.7 (2 s, CHo-C₆H₅), 129.6 (s, CHp-C₆H₅), 127.9/127.4 (2 s, CHm-C₆H₅), 91.0/90.9 (2 s, C₅H₅), 63.5/61.7 (2 s, CH), 20.0 (s, ReCH₂), 17.3/16.8 (2 s, CH₃); 31 P{ 1 H} (121 MHz) 21.1/21.0 (2 s, PPh₃, 48:52).

IR:¹ 1660 (ν_{NO} , s). MS:^{2a} 677 (53) [**6c**]⁺, 558 (100) [**6c**-NH₂CH(CH₃)(C₆H₅)]⁺.

4.1.9. $(S_{Re}S_C)/(R_{Re}S_C)-(\eta^5-C_5H_5)Re(NO)(PPh_3)(CH_2NHCH(CH_3)(C_6H_5)$ **(6c)**

The salt [**6c**-H]⁺ PF₆⁻ (0.0249 g, 0.325 mmol), THF (10 mL), and t-BuOK (0.0365 g, 0.325 mmol) were combined in a procedure analogous to that for **6a**. After 30 min, the solvent was removed by oil pump vacuum. Benzene (7 mL) was added, and the sample was filtered through a glass frit. Then hexanes (30 mL) were added to the filtrate with stirring. The mixture was kept at 4 °C. After 16 h, an orange powder precipitated, which was collected by filtration, washed with hexanes (2 × 4 mL), and dried by oil pump vacuum to give **6c** (0.100 g, 0.148 mmol, 40%; 48:52 diastereomer mixture).

NMR (δ in ppm). 1 H (400 MHz, 50:50 v/v $C_6D_6/CDCl_3$): 7.40–7.08 (m, 4 C_6H_5 , 20H), 4.83/4.81 (2 s, C_5H_5 , 5H, 48:52), 3.95–3.66 (m, ReC H_2 and CHCH $_3$, 3H), 1.31/1.27 (2 d, CH $_3$, 3H, 48:52); $^{13}C\{^1$ H} (101 MHz, CDCl $_3$): PPh $_3$ at 136.7/136.6 (2 d, 1 J(C,P) = 50.0 Hz, i), 130.0 (s, p), 122.7/133.7 (2 d, 2 J(C,P) = 11.0 Hz, o), 128.5/128.4 (2 d, 3 J(C,P) = 12.0 Hz, m); 129.9 (s, CHC $_6$ H $_5$), 127.6 (s, CHC $_6$ H $_5$), 127.2 (s, CHC $_6$ H $_5$), 90.0/89.9 (2 s, C_5 H $_5$), 61.7 (s, NCH), 25.6/23.6 (2 s, ReCH $_3$), 17.8/17.1 (2 s, CH $_2$); $^{31}P\{^{1}$ H} (162 MHz, C_6D_6): 27.2/26.9 (2 s, PPh $_3$).

IR: 1 1613 (v_{NO} , s).

4.1.10. $(R_{Re}S_C)$ - $[(\eta^5-C_5H_5)Re(NO)(PPh_3)(CH_2NH_2CH(CH_3)(C_6H_5))]^+$ $[BF_4^-]((R_{Re}S_C)$ -[6c- $H]^+$ $BF_4^-)$

A Schlenk was charged with (R)-1 (0.576 g, 1.03 mmol) [20] and CH₂Cl₂ (15 mL) and cooled to -78 °C. Then Ph₃C⁺ BF₄⁻ (0.370 g, 1.12 mmol) was added with stirring. After 30 min, (S)-1-phenylethyl amine (0.158 mL, 0.150 g, 1.24 mmol) was added. After 5 min, the cold bath was removed. After 1.5 h, the solvent was removed by oil pump vacuum. The residue was dissolved

in CH₂Cl₂ (5 mL). The solution was layered with diethyl ether (5 mL). After several hours, the yellow needles were collected by decantation, washed with diethyl ether (2 × 10 mL) and dried by oil pump vacuum. The mother liquor was layered with diethyl ether (15 mL) and kept for 12 h at room temperature. A second crop of yellow needles was similarly isolated. The crops were combined to give ($R_{\text{Re}}S_{\text{C}}$)-[$\mathbf{6c}$ -H]⁺ BF₄⁻ (0.610 g, 0.797 mmol, 77%). M.p. 141–142 °C, dec (capillary). Elemental Anal. Calc. for C₃₂H₃₃BF₄N₂OPRe: C, 50.20; H, 4.34; N, 3.66. Found: C, 49.92; H, 4.18; N, 3.46%.

NMR (CD₃CN, δ in ppm). ¹H (400 MHz): 7.48–7.21 (m, 4 C₆H₅, 20H), 6.47 (br s, NHH′, 1H), 6.11 (br s, NHH′, 1H), 5.11 (s, C₅H₅, 5H), 4.15–4.11 (m, CH, 1H), 3.79–3.77 (m, ReCHH′, 1H), 3.61–3.57 (m, ReCHH′, 1H), 1.55 (d, ³J(H,H′) = 6.8 Hz, CH₃, 3H); ¹³C{¹H} (101 MHz): PPh₃ at 135.2 (d, ¹J(C,P) = 53.0 Hz, *i*), 134.5 (d, ²J(C,P) = 11.0 Hz, *o*), 131.7 (s, *p*), 128.6 (d, ³J(C,P) = 11.0 Hz, *m*); 137.6 (s, CH(CH₃)C₆H₅), 130.2 (s, CH(CH₃)C₆H₅), 128.9 (s, CH(CH₃)C₆H₅), 91.6 (s, C₅H₅), 63.2 (s, CH), 19.1 (s, ReCH₂), 16.7 (s, CH₃); ³¹P{¹H} (162 MHz): 22.4 (s, PPh₃).

IR: 1 3227 (v_{NH} , m), 1660 (v_{NO} , s).

4.1.11. $[(\eta^5 - C_5 H_5)Re(NO)(PPh_3)(CH_2NH(CH_2CH_3)_2)]^+ PF_6^- ([\textbf{6d} - H]^+ PF_6^-)$

Complex **1** (0.123 g, 0.222 mmol), [20] CH_2Cl_2 (5 mL), Ph_3C^+ PF_6^- (0.0971 g, 0.244 mmol), diethyl amine (0.025 mL, 0.018 g, 0.25 mmol) were combined in a procedure analogous to that for [**6a**′-H]⁺ PF_6^- . As the solution warmed, a yellow powder precipitated, which was collected by filtration and washed with n-pentane (5 mL). The filtrate and washings were concentrated by oil pump vacuum (to ca. 2 mL). Then n-pentane (6 mL) was rapidly added. A yellow powder precipitated, which was collected by filtration and dried by oil pump vacuum. The two crops were combined to give [**6d**-H]⁺ $\text{PF}_6^-\text{CH}_2\text{Cl}_2$ (0.181 g, 0.219 mmol, 99%). M.p. 146–149 °C (capillary). Elemental Anal. Calc. for $\text{C}_{28}\text{H}_{33}\text{F}_6\text{N}_2\text{O}$ - $\text{P}_2\text{Re}\cdot\text{CH}_2\text{Cl}_2$ (82 7.2): C, 40.47; H, 4.10; N, 3.25. Found: C, 39.98; H, 4.03; N, 3.19%.

NMR (CD₂Cl₂, δ in ppm). ¹H (400 MHz): 7.47–7.44 (m, 3 C₆H₅, 9H), 7.32–7.28 (m, 3 C₆H₅, 6H), 5.31 (s, C₅H₅, 5H), 5.22 (br s, NH, 1H), 4.21 (d, ²J(H,H) = 13.2 Hz, ReCHH', 1H), 3.92–3.88 (m, NHCHH', 1H), 3.41–3.40 (m, NHCHH', 1H), 3.09–3.02 (m, ReCHH' and NHC'H₂, 3H), 1.19–1.12 (m, CH₃ and C'H₃), 6H); ¹³C{¹H} (101 MHz): PPh₃ at 134.5 (d, ¹J(C,P) = 53.7 Hz, *i*), 133.7 (d, ²J(C,P) = 10.9 Hz, o), 131.2 (s, p), 129.2 (d, ³J(C,P) = 10.2 Hz, m); 91.0 (s, C₅H₅), 51.6, 48.0 (2 s, NCH₂ and NC'H₂), 28.3 (s, ReCH₂), 8.79, 7.96 (2 s, CH₃ and C'H₃); ³¹P{¹H} (162 MHz): 21.3 (s, PPh₃), –148.4 (sep, ¹J(P,F) = 712 Hz, PF₆).

IR:¹ 1629 (v_{NO} , s). MS:^{2a} 631 (29) [**6d**-H]⁺, 558 (100) [**6d**-NH(CH₂CH₃)₂]⁺.

4.1.12. $(\eta^5 - C_5H_5)Re(NO)(PPh_3)(CH_2N(CH_2CH_3)_2)$ (**6d**)

The salt [**6d**-H]⁺ PF₆⁻ (0.103 g, 0.132 mmol), THF (5 mL), and t-BuOK (0.0222 g, 0.198 mmol) were combined in a procedure analogous to that for **6a**. An identical workup gave **6d** as an orange powder (0.0710 g, 0.113 mmol, 85%). M.p. 69–71 °C, dec (capillary). Elemental Anal. Calc. for $C_{28}H_{32}N_2OPRe$ (629.7): C, 53.40; H, 5.12; N, 4.45. Found: C, 53.83; H, 5.41; N, 4.10%.

NMR (C_6D_6 , δ in ppm). 1 H (400 MHz): 7.73–7.51 (m, 3 C_6H_5 , 6H), 7.04–6.95 (m, 3 C_6H_5 , 9H), 4.81 (s, C_5H_5 , 5H), 3.99–3.96 (m, ReCHH', 1H), 3.79–3.74 (m, ReCHH', 1H), 3.14–3.09, 2.57–2.52 (2 m, NCH₂ and NC'H₂, 2 × 2H), 1.15–1.11 (m, 2 CH₃, 6H); 13 C{ 1 H} (101 MHz): PPh₃ at 137.5 (d, 1 J(C,P) = 50.9 Hz, i), 134.1 (d, 2 J(C,P) = 10.8 Hz, o), 130.2 (s, p), 128.5 (d, 3 J(C,P) = 10.2 Hz, m); 91.1 (s, C_5 H₅), 49.8 (s, NCH₂), 25.7 (s, ReCH₂), 12.9 (s, CH₃); 31 P{ 1 H} (162 MHz): 26.2 (s, PPh₃).

IR: 1 1622 (ν_{NO} , s). MS: 2a 629 (6) [**6d**] $^{+}$, 558 (100) [**6d**-N(CH₂CH₃)₂] $^{+}$.

4.1.13. $[(\eta^5 - C_5H_5)Re(NO)(PPh_3)(CH_2NH(CH_2CH_2CH_2CH_3)_2)]^+ PF_6^- ([\textbf{6e}-H]^+ PF_6^-)$

Complex **1** (0.505 g, 0.904 mmol), [20] CH_2Cl_2 (5 mL), Ph_3C^+ PF_6^- (0.385 g, 0.994 mmol), and di-*n*-butyl amine (0.170 mL, 0.129 g, 0.994 mmol) were combined in a procedure analogous to that for [**6a**′-H]⁺ PF_6^- . A similar workup (sample concentration to ca. 2 mL; addition of 10 mL of *n*-pentane; washing with 2 × 4 mL of *n*-pentane) gave [**6e**-H]⁺ PF_6^- (0.606 g, 0.729 mmol, 81%) as a yellow powder. M.p. 142–150 °C, dec (capillary). Elemental Anal. Calc. for $\text{C}_{32}\text{H}_{41}\text{F}_6\text{N}_2\text{OP}_2\text{Re}$ (832): C, 46.20; H, 4.97; N, 3.37. Found: C, 46.28; H, 5.10; N, 3.27%.

NMR (CD₂Cl₂, δ in ppm). 1 H (400 MHz): 7.75–7.46 (m, 3 C₆H₅, 6H), 7.34–7.29 (m, 3 C₆H₅, 9H), 5.24 (s, C₅H₅, 5H), 5.04 (br s, NH, 1H), 4.25 (d, 2 J(H,H) = 13.1 Hz, ReCHH′, 1H), 3.98–3.96 (m, NHCHH′, 1H), 3.23–3.21 (m, ReCHH′, 1H), 2.98–2.93 (m, NC′HH′ and NHCHH′, 3H), 1.45–1.29 (m, CH₂CH₂ and CH′₂CH′₂, 8H), 0.97–0.91 (m, CH₃ and CH′₃, 6H); 13 C{ 1 H} (101 MHz): PPh₃ at 134.6 (d, 1 J(C,P) = 54.2 Hz, i), 133.6 (d, 2 J(C,P) = 10.7 Hz, o), 131.3 (s, p), 129.3 (d, 3 J(C,P) = 10.3 Hz, m); 91.0 (s, C₅H₅), 57.6 (s, NCH₂), 29.9 (s, ReCH₂), 26.4, 24.6 (2 s, NCH₂CH₂ and NCH₂C'H₂), 20.3 (s, NCH₂CH₂CH₂), 13.8, 13.7 (2 s, CH₃ and C'H₃); 31 P{ 1 H} (162 MHz): 22.3 (s, PPh₃), –143.8 (sep, 1 J(P,F) = 707 Hz, PF₆).

IR: 1 1625 (ν_{NO} , s). MS: 2a 685 (3) [**6e**-H]⁺, 558 (100) [**6e**-NH(CH₂CH₂CH₂CH₃)₂]⁺.

4.1.14. $(\eta^5 - C_5H_5)Re(NO)(PPh_3)(CH_2N(CH_2CH_2CH_2CH_3)_2)$ (**6e**)

A Schlenk flask was charged with $[\mathbf{6e}\text{-H}]^+$ PF₆ $^-$ (0.200 g, 0.240 mmol) and THF (5 mL). Then t-BuOK (0.0290 g, 0.264 mmol) was added with stirring. After 1 h, the solvent was removed from the nearly homogeneous mixture by oil pump vacuum. Then n-pentane (7 mL) was added, and the sample was filtered through a glass frit. The solvent was removed from the filtrate by oil pump vacuum to give $\mathbf{6e}$ as an orange powder (0.161 g, 0.194 mmol, 98%). M.p. $107\text{-}108\,^{\circ}\text{C}$ (capillary). Elemental Anal. Calc. for $\text{C}_{32}\text{H}_{40}\text{N}_2\text{OPRe}$ (686): C, 56.02; H, 5.87; N, 4.08. Found: C, 55.51; H, 5.84; N, 3.79%.

NMR (δ in ppm). 1 H (400 MHz, C_6D_6): 7.88–7.62 (m, 3 C_6H_5 , 6H), 7.27–7.08 (m, 3 C_6H_5 , 9H), 4.99 (s, C_5H_5 , 5H), 4.19–4.17 (m, ReCHH', 1H), 4.00–3.96 (m, ReCHH', 1H), 3.21–3.18, 2.60–2.57 (2 m, NCH₂ and NC'H₂. 2 × 2H), 1.74–1.58 (m, NCH₂CH₂CH₂ and NC'H₂C'H₂C'H₂, 2 × 4H), 1.15–1.11 (m, 2 CH₃, 6H); 13 C{ 1 H} (101 MHz, CD₂Cl₂): PPh₃ at 136.9 (d, 1 J(C,P) = 51.1 Hz, i), 133.9 (d, 2 J(C,P) = 10.7 Hz, o), 130.3 (s, p), 128.6 (d, 3 J(C,P) = 10.0 Hz, m); 90.9 (s, C_5 H₅), 56.3 (s, NCH₂), 30.2 (s, ReCH₂), 27.1 (s, NCH₂CH₂), 21.4 (s, NCH₂CH₂CH₂), 14.5 (s, CH₃); 31 P{ 1 H} (162 MHz, C_6 D₆): 27.3 (s, PPh₃).

IR (powder film, cm $^{-1}$): 1 1625 (ν_{NO} , s). MS: 2a 687 (11) [**6e**] $^{+}$, 558 (100) [**6e**–NH(CH $_{2}$ CH $_{2}$ CH $_{2}$ CH $_{3}$) $_{2}$] $^{+}$.

4.1.15. $[(\eta^5 - C_5H_5)Re(NO)(PPh_3)(CH_2NH(CH_2C_6H_5)_2)]^+ PF_6^- ([\textbf{6f}-H]^+ PF_6^-)$

Complex **1** (0.500 g, 0.895 mmol), [20] CH_2Cl_2 (5 mL), Ph_3C^+ PF_6^- (0.382 g, 0.985 mmol), and dibenzyl amine (0.25 mL; 0.19 g, 0.99 mmol) were combined in a procedure analogous to that for [**6a**′-H]⁺ PF_6^- . A similar workup (sample concentration to ca. 2 mL; addition of 10 mL of benzene) gave [**6f**-H]⁺ PF_6^- (0.799 g, 0.887 mmol, 99%) as a yellow powder. M.p. 121–129 °C, dec (capillary). Elemental Anal. Calc. for $C_{38}H_{37}F_6N_2OP_2Re$ (900): C, 50.71; H, 4.14; N, 3.11. Found: C, 50.65; H, 4.16; N, 3.14%.

NMR (CD₂Cl₂, δ in ppm). 1 H (400 MHz): 7.77–7.51 (m, 5 C₆H₅, 16H), 7.40–7.26 (m, 5 C₆H₅, 9H), 4.95 (s, C₅H₅, 5H), 4.85 (d, 2 J(H,H) = 13.3 Hz, ReCHH', 1H), 4.38–4.34, 4.06–4.04 (2 m, NHCH₂ and NHC'H₂, 2 × 2H), 3.66–3.64 (m, ReCHH', 1H); 13 C{ 1 H} (101 MHz): PPh₃ at 134.2 (d, 1 J(C,P) = 54.2 Hz, i), 133.6 (d, 2 J(C,P) = 10.8 Hz, o), 131.4 (d, 4 J(C,P) = 1.7 Hz, p), 129.3 (d, 3 J(C,P) = 10.3 Hz, m); CPh and CPh at 131.3, 131.1, 130.9, 130.6,

130.5, 130.0, 129.9, 129.8; 91.0 (s, C_5H_5), 60.8, 58.6 (2 s, NCH₂ and NC'H₂), 28.6 (s, ReCH₂); ³¹P{¹H} (162 MHz): 20.1 (s, PPh₃), –142.9 (sep, ¹J(P,F) = 707 Hz, PF₆).

IR:¹ 1637 (ν_{NO} , s). MS:^{2a} 755 (10) [**6f**-H]⁺, 679 (13) [**6f**-C₆H₅]⁺, 558 (100) [**6f**-NH(CH₂C₆H₅)₂]⁺.

4.1.16. $(\eta^5 - C_5H_5)Re(NO)(PPh_3)(CH_2N(CH_2C_6H_5)_2)$ (**6f**)

The salt [**6f**-H] $^+$ PF $_6^-$ (0.300 g, 0.330 mmol), THF (7 mL) and t-BuOK (0.0380 g, 0.340 mmol) were combined in a procedure analogous to that given for **6a**. An identical workup gave **6f** as an orange powder (0.197 g, 0.219 mmol, 99%). M.p. 174–176 °C, dec (capillary). Elemental Anal. Calc. for $C_{38}H_{36}N_2OPRe$ (754): C, 60.53; H, 4.81; N, 3.71. Found: C, 60.88; H, 4.97; N, 3.64%.

NMR (C_6D_6 , δ in ppm). ¹H (400 MHz): 7.45–7.41 (m, 5 C_6H_5 , 10H), 7.22–7.11 (m, 5 C_6H_5 , 6H), 7.04–6.97 (m, 5 C_6H_5 , 9H), 4.67 (s, C_5H_5 , 5H), 4.55, 3.01 (2 d, ²J(H,H) = 13.0 Hz, NC H_2 and NC' H_2 , 2 × 2H), 4.08–4.04 (m, ReCHH', 1H), 3.48–3.43 (m, ReCHH', 1H); ¹³C{¹H} (101 MHz): PPh₃ at 136.9 (d, ¹J(C,P) = 50.8 Hz, *i*), 134.0 (d, ²J(C,P) = 10.8 Hz, *o*), 130.2 (s, *p*), 128.6 (d, ³J(C,P) = 10.3 Hz, *m*); CPh at 142.7, 129.9, 128.8, 126.7; 90.8 (s, C_5H_5), 62.2, 27.6 (2 s, NCH₂ and NC'H₂), 30.6 (s, ReCH₂); ³¹P{¹H} (162 MHz): 25.1 (s, PPh₃).

IR:¹ 1625 (ν_{NO} , s). MS:^{2a} 753 (11) [**6f**-H]⁺, 679 (13) [**6f**-C₆H₅]⁺, 558 (100) [**6f**-NH(CH₂C₆H₅)₂]⁺.

4.1.17. $[(\eta^5 - C_5H_5)Re(NO)(PPh_3)(CH_2\overline{NHCH_2CH_2CH_2CH_2})]^+ PF_6^- ([\mathbf{6g} - H]^+ PF_6^-)$

Complex **1** (1.006 g, 1.800 mmol), [20] CH_2Cl_2 (10 mL), Ph_3C^+ PF_6^- (0.769 g, 1.98 mmol), and pyrrolidine (0.18 mL, 0.15 g, 2.2 mmol) were combined in a procedure analogous to that for [**6a**′-H]⁺ PF_6^- . A similar workup (1.5 h at room temperature; sample concentration to ca. 5 mL; addition of 50 mL of n-pentane; 3 d before filtration) gave [**6g**-H]⁺ PF_6^- (1.393 g, 1.800 mmol, >99%) as a yellow powder. M.p. 180–182 °C, dec (capillary). Elemental Anal. Calc. for $\text{C}_{28}\text{H}_{31}\text{F}_6\text{N}_2\text{OP}_2\text{Re}$ (773.71): C, 43.47; H, 4.04; N, 3.62. Found: C, 43.21; H, 4.08; N, 3.88%.

NMR (CD₃CN, δ in ppm). 1 H (400 MHz): 7.52–7.45 (m, 3 C₆H₅, 9H), 7.35–7.29 (m, 3 C₆H₅, 6H), 6.15 (br s, NH, 1H), 5.24 (s, C₅H₅, 5H), 4.33 (d, 2 J(H,H') = 13.2 Hz, ReCHH', 1H,), 3.92–3.88 (m, ReCHH', 1H), 3.69–3.67, 3.57–3.53, 2.73–2.71 (3 m, NCHH' and NC'HH', 1H, 1H, and 2H), 1.95–1.91 (m, NHCH₂CH₂CH₂, 4H, obscured by CD₃CN); 13 C{ 1 H} (101 MHz): PPh₃ at 135.3 (d, 1 J(C,P) = 53.4 Hz, i), 134.3 (d, 2 J(C,P) = 10.7 Hz, o), 131.8 (d, 4 J(C,P) = 1.5 Hz, p), 129.8 (d, 3 J(C,P) = 10.7 Hz, m); 91.8 (s, C₅H₅), 60.7, 56.9 (2 s, NCH₂ and NC'H₂), 29.9 (s, ReCH₂), 24.3, 23.4 (2 s, NCH₂CH₂ and NCH₂C'H₂); 31 P{ 1 H} (162 MHz): 23.1 (s, PPh₃), $^{-1}$ 42.5 (sep, 1 J(P,F) = 703 Hz, PF₆).

IR:¹ 1633 (v_{NO} , s). MS:^{2a} 627 (11) [**6g**-H]⁺, 558 (100) [**6g**-C₄H₈NH]⁺, 366 (22) [**6g**-PPh₃]⁺.

4.1.18. (S)-[$(\eta^5$ - C_5H_5)Re(NO)(PPh₃)(CH₂NHCH₂CH₂CH₂CH₂CH₂)]⁺ PF₆⁻ ((S)-[**6g**-H]⁺ PF₆⁻)

A Schlenk flask was charged with (*S*)-**1** (0.135 g, 0.242 mmol) [20] and CH_2Cl_2 (4 mL), and cooled to -78 °C. Then Ph_3C^+ PF_6^- (0.103 g, 0.266 mmol) was added with stirring. After 30 min, pyrrolidine (0.022 mL; 0.019 g, 0.27 mmol) was added. After 20 min, the cold bath was removed. After 30 min, the mixture was concentrated by oil pump vacuum (to ca. 2 mL), and a few drops of ethanol were added. This sample was added dropwise to a stirred solution of n-pentane (15 mL). A yellow precipitate formed immediately, which was collected by filtration, washed with n-pentane (2 × 5 mL), and dried by oil pump vacuum to give (*S*)-[**6g**-H]⁺ PF_6^- CH₂Cl₂ (0.173 g, 0.199 mmol, 82%). M.p. 125–127 °C, dec (capillary). Elemental Anal. Calc. for $C_{28}H_{31}F_6N_2OP_2Re$ CH₂Cl₂ (773.7): C, 40.57; H, 3.87; N, 3.26. Found: C, 40.50; H, 3.99; N, 3.07%; $[\alpha]_{25}^{589} = 136^\circ \pm 1^\circ$ (c = 1.00 mg mL⁻¹, CH_2Cl_2). The NMR, IR, and

mass spectra were similar to those of the racemate, and are given elsewhere [17].

4.1.19.
$$(\eta^5 - C_5H_5)Re(NO)(PPh_3)(CH_2NCH_2CH_2CH_2CH_2)$$
 (**6g**)

A Schlenk flask was charged with $[\mathbf{6g}\text{-H}]^+$ PF $_6^-$ (0.336 g, 0.434 mmol) and toluene (15 mL) and cooled to -78 °C. Then t-BuOK (1.0 M in THF; 0.52 mL, 0.52 mmol) was added with stirring. The cold bath was removed. After 30 min, the mixture was filtered through a Celite plug (4 × 2 cm). The Celite was rinsed with toluene (3 × 5 mL). The filtrate and rinsings were concentrated by oil pump vacuum (to ca. 4 mL). Then n-pentane (10 mL) was added. After 21 h at -78 °C, the supernatant was decanted from an orange precipitate, which was dried by oil pump vacuum to give $\mathbf{6g}$ (0.224 g, 0.357 mmol, 82%). M.p. 130–132 °C, dec (capillary). Elemental Anal. Calc. for $C_{28}H_{30}N_2$ OPRe (627.74): C, 53.57; H, 4.82; N, 4.46. Found: C, 53.70; H, 4.79; N, 4.25.

NMR (C_6D_6 , δ in ppm). 1H (400 MHz): 7.76–7.36 (m, 3 C_6H_5 , 6H), 7.12–6.95 (m, 3 C_6H_5 , 9H), 4.82 (s, C_5H_5 , 5H), 4.20 (d, 2J (H,H') = 11.5 Hz, ReCHH', 1H), 3.72 (dd, 2J (H,H') = 11.5 Hz, 3J (H,P) = 7.6 Hz, ReCHH', 1H), 2.92–2.90 (m, NCH₂, 2H), 2.70–2.68 (m, NCH'₂, 2H), 1.82–1.81 (m, CH₂CH₂, 4H); $^{13}C_1^{1}H$ } (101 MHz): PPh₃ at 137.3 (d, 1J (C,P) = 49.6 Hz, i), 133.9 (d, 2J (C,P) = 11.0 Hz, o), 129.9 (s, p), 128.4 (d, upfield peak obscured by C_6D_6 , m); 90.7 (s, C_5H_5), 58.5 (s, NCH₂), 26.3 (s, ReCH₂), 25.0 (s, CH₂CH₂); $^{31}P_1^{1}H$ } (162 MHz): 26.8 (s, PPh₃).

IR:¹ 1617 (ν_{NO} , s). MS:^{2a} 629 (11) [**6g**]⁺, 558 (100) [**6g**-C₄H₈N]⁺, 366 (18) [**6g**-PPh₃]⁺.

$4.1.20.~(S) - (\eta^5 - C_5H_5)Re(NO)(PPh_3)(CH_2 \underset{NCH_2CH_2CH_2}{\square} CH_2) ((S) - \textbf{6g})$

A Schlenk flask was charged with (S)-[**6g**-H]⁺ PF₆⁻ (0.0903 g, 0.117 mmol) and THF (4 mL). Then t-BuOK (0.0196 g, 0.175 mmol) was added with stirring. After 30 min, the solvent was removed from the nearly homogeneous mixture by oil pump vacuum. Then benzene/pentane (3:1 v/v, 10 mL) was added, and the sample was filtered through a Celite plug. The solvent was removed from the filtrate by oil pump vacuum to give (S)-**6g**-n-pentane as an orange powder (0.0732 g, 0.107 mmol, 89%). M.p 131–130 °C, dec (capillary). Elemental Anal. Calc. for C₂₈H₃₀N₂OPRe·n-pentane (700.3): C, 56.63; H, 6.05; N, 4.00. Found: C, 56.87; H, 5.84; N, 3.86%; [α]₂₅⁵⁸⁹ = 173° ± 2° (c = 1.00 mg mL⁻¹, CH₂Cl₂). The NMR, IR, and mass spectra were similar to those of the racemate, and are given elsewhere [17].

4.1.21. $[(\eta^5 - C_5H_5)Re(NO)(PPh_3)(CH_2NHCH_2CH_2CH_2CH_2)]^+ PF_6^- ([\mathbf{6h}-H]^+ PF_6^-)$

Complex **1** (0.390 g, 0.698 mmol), [20] CH_2Cl_2 (6 mL), Ph_3C^+ PF_6^- (0.298 g, 0.768 mmol), and piperidine (0.076 mL, 0.065 g, 0.77 mmol) were combined in a procedure analogous to that for [**6a**′-H]⁺ PF_6^- . The cold bath was removed. After 1 h, the yellow powder was collected by filtration, washed with n-pentane (2 × 4 mL), and dried by oil pump vacuum to give [**6h**-H]⁺ PF_6^- ·CH $_2\text{Cl}_2$ (0.583 g, 0.667 mmol, 96%). M.p. 148–151 °C, dec (capillary). Elemental Anal. Calc. for $\text{C}_{29}\text{H}_{33}\text{F}_6\text{N}_2\text{OP}_2\text{Re}\cdot\text{CH}_2\text{Cl}_2$ (873.7): C, 41.29; H, 4.13; N, 3.73. Found: C, 41.10; H, 4.31; N, 3.25%.

NMR (CD₂Cl₂, δ in ppm). 1 H (400 MHz): 7.67–7.46 (m, 3 C_6H_5 , 9H), 7.33–7.28 (m, 3 C_6H_5 , 6H), 5.26 (s, C_5H_5 , 5H), 4.90 (br s, NH, 1H), 4.28 (d, 2 J(H,H) = 12.9 Hz, ReCHH', 1H), 4.04–4.00, 3.83–3.80 (2 m, NHCHH' and NHCHH', 2 × 1H), 3.54–3.50 (m, ReCHH', 1H), 2.59–2.57 (m, NHC'HH', 1H), 2.50–2.47 (m, NHC'HH', 1H), 1.90–1.87 (m, NHCH₂CH₂, 2H), 1.84–1.80 (m, NHC'H₂C'H'₂, 2H), 1.73–1.70 (m, NHCH₂CH₂CH₂, 2H); 13 C{ 1 H} (101 MHz): PPh₃ at 134.5 (d, 1 J(C,P) = 54.1 Hz, i), 133.6 (d, 2 J(C,P) = 10.8 Hz, o), 131.3 (s, p), 129.2 (d, 3 J(C,P) = 10.3 Hz, m); 91.0 (s, C_5 H₅), 54.3, 53.3 (2 s, NCH₂ and NC'H₂), 30.9 (s, ReCH₂), 23.9, 22.8 (2 s, NC'H₂CH₂ and

 NCH_2CH_2), 22.3 (s, $NCH_2CH_2CH_2$); $^{31}P\{^{1}H\}$ (162 MHz): 20.2 (s, PPh_3), -145.1 (sep, $^{1}J(P,F) = 710$ Hz, PF_6).

IR: 1 1633 (v_{NO} , s). MS: 2a 644 (14) [**6h**-H] $^+$, 558 (100) [**6h**-NHCH $_2$ CH $_2$ CH $_2$ CH $_2$ CH $_2$] $^+$.

$4.1.22.\ (\eta^5\text{-}C_5H_5)Re(NO)(PPh_3)(CH_2NCH_2CH_2CH_2CH_2CH_2)\ (\textbf{6h})$

The salt [**6h**-H]⁺ PF₆⁻ (0.176 g, 0.225 mmol), THF (7 mL), and t-BuOK (0.0378 g, 0.337 mmol) were combined in a procedure analogous to that given for **6a**. An identical workup gave **6h** as an orange powder (0.140 g, 0.218 mmol, 97%). M.p. 179–185 °C, dec (capillary). Elemental Anal. Calc. for $C_{29}H_{32}N_2OPRe$ (641.7): C, 54.27; H, 5.03; N, 4.37. Found: C, 54.33; H, 5.45; N, 4.17%.

NMR (CD₂Cl₂, δ in ppm). ¹H (400 MHz): 7.41–7.37 (m, 3 C₆H₅, 15H), 4.99 (s, 3 C₅H₅, 5H), 3.75 (d, ²J(H,H) = 11.8 Hz, ReCHH', 1H), 3.47–3.42 (m, ReCHH', 1H), 2.54–2.51, 2.13–2.11 (2 m, 2 NCH₂, 2 × 2H), 1.56–1.43 (m, 2 NCH₂CH₂, 4H), 1.36–1.33 (m, NCH₂CH₂CH₂, 2H); ¹³C{¹H} (101 MHz): PPh₃ at 136.8 (d, ¹J(C,P) = 51.5 Hz, *i*), 134.0 (d, ²J(C,P) = 10.7 Hz, *o*), 130.4 (s, *p*), 128.6 (d, ³J(C,P) = 13.6 Hz, *m*); 91.0 (s, C₅H₅), 57.7 (s, NCH₂), 31.6 (s, ReCH₂), 27.1 (s, NCH₂CH₂), 25.1 (s, NCH₂CH₂CH₂); ³¹P{¹H} (162 MHz): 26.1 (s, PPh₃).

IR:¹ 1625 (v_{NO} , s). MS:^{2a} 641 (9) [**6h**]⁺, 558 (100) [**6h**-NCH₂CH₂CH₂CH₂CH₂]⁺.

4.1.23. $(S_{Re}R_{N},R_{Re}S_{N})/(S_{Re}S_{N},R_{Re}R_{N})-[(\eta^{5}-C_{5}H_{5})Re(NO)(PPh_{3})-(CH_{2}NH(CH_{3})CH_{2}CH_{2}OH)]^{+}PF_{6}^{-}([\textbf{6i}-H]^{+}PF_{6}^{-})$

Complex **1** (0.105 g, 0.188 mmol), [20] CH₂Cl₂ (5 mL), Ph₃C⁺ PF₆⁻ (0.0804 g, 0.207 mmol), and methyl 2-hydroxyethyl amine (0.017 mL, 0.016 g, 0.21 mmol) were combined in a procedure analogous to that for [**6a**′-H]⁺ PF₆⁻. A similar workup (sample concentration to ca. 2 mL; addition of 10 mL of n-pentane; washing with 2×4 mL of n-pentane) gave [**6i**-H]⁺ PF₆⁻ (0.137 g, 0.176 mmol, 93%) as a yellow powder and 75:25 diastereomer mixture. M.p. 102-103 °C (capillary). Elemental Anal. Calc. for $C_{27}H_{31}F_6N_2O_2P_2Re$ (777.7): C, 41.70; H, 4.02; N, 3.60. Found: C, 41.46; H, 4.04; N, 3.53%.

NMR (CD₂Cl₂, δ in ppm). 1 H (400 MHz): 7.48–7.47 (m, 3 C₆H₅, 9H), 7.33–7.21 (m, 3 C₆H₅, 6H), 5.31/5.27 (2 s, C₅H₅, 5H, 75:25), 4.54/4.48 (2 d, 2 J(H,H) = 12.8 Hz, ReCHH', 1H, 75:25), 4.12 (br s, OH, 1H), 3.89–3.73 (m, CH₂OH and ReCHH', 3H), 3.31–3.28 (m, NCHH', 1H), 3.05–3.02 (m, NCHH', 1H), 2.85 (s, NCH₃, 3H); 13 C{ 1 H} (101 MHz): PPh₃ at 134.4 (d, 1 J(C,P) = 54.2 Hz, *i*), 133.7 (d, 2 J(C,P) = 10.6 Hz, *o*), 131.4 (s, *p*), 129.3 (d, 3 J(C,P) = 10.5 Hz, *m*); 91.2 (s, C₅H₅), 62.8/58.4 (2 s, CH₂OH), 56.4 (s, NCH₃), 46.1/43.5 (2 s, NCH₂), 31.9 (s, ReCH₂); 31 P{ 1 H} (162 MHz): 22.2/21.7 (2 s, PPh₃, 75:25), –143.1 (sep, 1 J(P,F) = 707 Hz, PF₆).

IR: 1 1644 (ν_{NO} , s). MS: 2a 631 (9) [**6i**-H]⁺, 558 (100) [**6i**-NH(CH₃)(CH₂CH₂OH)]⁺.

4.1.24. $(\eta^5 - C_5H_5)Re(NO)(PPh_3)(CH_2N(CH_3)CH_2CH_2OH)$ (**6i**)

The salt [$\mathbf{6i}$ -H] $^+$ PF $_6^-$ (0.128 g, 0.203 mmol), THF (5 mL), and t-BuOK (0.0342 g, 0.304 mmol) were combined in a procedure analogous to that for $\mathbf{6a}$. An identical workup gave $\mathbf{6i}$ as an orange-yellow powder (0.127 g, 0.201 mmol, 99%). M.p. 132–136 °C (capillary). Elemental Anal. Calc. for $C_{27}H_{30}N_2O_2$ PRe (631.7): C, 51.33; H, 4.79; N, 4.43. Found: C, 51.91; H, 5.20; N, 3.80%⁵.

NMR (C_6D_6 , δ in ppm). 1 H (300 MHz): 7.50–7.44 (m, 3 C_6H_5 , 6H), 7.05–6.93 (m, 3 C_6H_5 , 9H), 4.73 (s, C_5H_5 , 5H), 3.93 (d, 2 J(H,H) = 11.8 Hz, ReCHH', 1H), 3.83–3.76 (m, ReCHH', 1H), 3.65–3.61 (m, CH_2OH), 3.00–2.92 (m, NCH_2 , 2H), 2.46 (s, NCH_3 , 3H), 2.35–2.28 (m, OH, 1H); $^{13}C_1^{13}$ H (76 MHz): PPh_3 at 136.8 (d, 1 J(C_7 P) = 51.3 Hz, i), 133.8 (d, 2 J(C_7 P) = 10.6 Hz, o), 130.5 (d,

 $^{^5}$ This microanalysis poorly or marginally agrees with the empirical formula, but it is nonetheless reported as the best obtained to date. The NMR spectra indicate high purities ($\geq 98\%$).

 $^{4}J(C,P) = 2.0 \text{ Hz}, p), 128.4 \text{ (d, }^{3}J(C,P) = 14.3 \text{ Hz}, m); 90.4 \text{ (s, } C_{5}H_{5}),$ 62.8 (s, CH_2OH), 58.4 (s, NCH_3), 44.8 (s, NCH_2), 30.5 (s, $ReCH_2$); ³¹P {¹H} (121 MHz): 26.8 (s, *PPh*₃).

IR:¹ 1617 (v_{NO} , s). MS:^{2a} 631 (100) [**6i**]⁺, 558 (87) [**6i**– $N(CH_3)(CH_2CH_2OH)]^+$.

Crystallography. A. Complex [4a-H]⁺ CF₃SO₃⁻ was dissolved in CH₂Cl₂ and layered with hexane. After 5 d at 4 °C, yellow prisms of [4a-H]⁺ CF₃SO₃ - were collected. Data were collected using a Nonius KappaCCD area detector as outlined in Table 1. Cell parameters were obtained from 10 frames using a 10° scan and refined with 6734 reflections. Lorentz, polarization, and absorption corrections were applied [38]. The space group was determined from systematic absences and subsequent least-squares refinement. The structure was solved by direct methods. The parameters were refined with all data by full-matrix-least-squares on F² using SHELXL-97 [39]. Non-hydrogen atoms were refined with anisotropic thermal parameters. The hydrogen atoms were fixed in idealized positions using a riding model. Scattering factors were taken from literature

B. Complex [4b-H]⁺ CF₃SO₃⁻ was prepared as described earlier [4], crystallized from toluene/hexane, and analyzed as described for [4a-H]⁺ CF₃SO₃⁻ (cell parameters from 10 frames using a 10° scan; refined with 13624 reflections). The structure was solved and refined as described for [4a-H]+ CF₃SO₃-. The unit cell contained two sets of two independent salt molecules, with the cations of each set having identical configurations at rhenium.

C. Complex $[6a'-H]^+$ PF₆⁻ was dissolved in CH₂Cl₂ and layered with benzene. After 4 d at 4 °C, orange prisms of [6a'-H]+ $PF_6^- \cdot (CH_2Cl_2)_{0.5} \cdot (C_6H_6)_{0.5}$ were collected and analyzed as described for [4a-H]⁺ CF₃SO₃⁻ (cell parameters from 10 frames using a 10° scan; refined with 7963 reflections). The CH₂Cl₂ molecule showed displacement disorder (C200; 50:50 occupancy about an inversion center).

D. Complex [6d-H]⁺ PF₆⁻ was dissolved in CH₂Cl₂ and layered with n-pentane. After 3 d at 20 °C, orange prisms of [6d-H]⁺ PF₆--CH₂Cl₂ were collected and analyzed as described for [**4a**-H] CF₃SO₃ (cell parameters from 10 frames using a 10° scan; refined with 7410 reflections). The structure was solved and refined as described for [**4a**-H] CF₃SO₃⁻.

E. Complex [6f-H]* PF₆- was dissolved in CH₂Cl₂ and layered with benzene. After 2 d at 4 °C, orange prisms of [6f-H]+ PF₆⁻·(CH₂Cl₂)_{1.5} were collected and analyzed as described for [4a-H]⁺ CF₃SO₃⁻ (cell parameters from 10 frames using a 10° scan; refined with 8913 reflections). The structure was solved and refined as described for [4a-H]⁺ CF₃SO₃⁻. One CH₂Cl₂ molecule showed displacement disorder (C200-Cl21; 50:50 occupancy about an inver-

F. Complex [6h-H]⁺ PF₆⁻ was dissolved in CH₂Cl₂ and layered with benzene. After 2 d at 4 °C, orange prisms of [6h-H]+ PF₆--CH₂Cl₂ were collected and analyzed as described for [4a-H]⁺ CF₃SO₃⁻ (cell parameters from 10 frames using a 10° scan; refined with 7341 reflections). The structure was solved and refined as described for [4a-H]⁺ CF₃SO₃⁻. One CH₂Cl₂ molecule exhibited displacement disorder (C100/Cl11/Cl12, C101/Cl13/Cl14), which refined to a 60:40 occupancy ratio.

G. Complex $(R_{Re}S_C)$ -**6c** was generated as described in the text, and dissolved in n-pentane and layered with CH₂Cl₂. After 3 d at room temperature, orange prisms of $(R_{Re}S_C)$ -6c were collected and analyzed as described for [4a-H]⁺ CF₃SO₃⁻ (cell parameters were from 10 frames using a 10° scan; refined from 15 reflections). The structure was solved and refined as described for [4a-H]+ CF₃SO₃⁻. The absolute configuration was confirmed by Flack's test (absolute structure parameter -0.024(14); theory for correct and inverted structures, 0 and 1) [41].

H. Complex 6f was dissolved in CH₂Cl₂ and layered with n-pentane. After 2 h at 20 °C, orange prisms of 6f were collected and ana-

lyzed as described for [4a-H]⁺ CF₃SO₃⁻ (cell parameters from 10 frames using a 10° scan; refined with 7042 reflections). The structure was solved and refined as described for [4a-H]+ CF₃SO₃-.

Supporting information available

CIF files with crystallographic data for [4a,b-H]⁺ CF₃SO₃⁻, [6a'-H]⁺ $PF_6^- \cdot (CH_2Cl_2)_{0.5} \cdot (C_6H_6)_{0.5}$, $[6d-H]^+$ $PF_6^- \cdot CH_2Cl_2$, $PF_6^- \cdot (CH_2Cl_2)_{1.5}$, $[6h-H]^+ PF_6^- \cdot CH_2Cl_2$, $(R_{Re}S_C)-6c$, and 6f.

Acknowledgment

We thank the Deutsche Forschungsgemeinschaft (DFG, GL 300/ 8-1 (SPP 1179) and postdoctoral fellowship to O.M.) and the US National Science Foundation (CHE-9408980, CHE-0719267) for support.

References

- [1] G.B. Kauffman, Coord. Chem. Rev. 12 (1974) 105-149.
- (a) T.B. Gunnoe, Eur. J. Inorg. Chem. 1185 (2007), and references therein; (b) C. Munro-Leighton, Y. Feng, J. Zhang, N.M. Alsop, T.B. Gunnoe, P.D. Boyle, J.L. Peterson, Inorg. Chem. 47 (2008) 6124.
- [3] (a) J.R. Fulton, S. Sklenak, M.W. Bouwkamp, R.G. Bergman, J. Am. Chem. Soc. 124 (2002) 4722;
 - (b) A.W. Holland, R.G. Bergman, J. Am. Chem. Soc. 124 (2002) 14684;
- (c) D.J. Fox, R.G. Bergman, Organometallics 23 (2004) 1656;(d) D. Rais, R.G. Bergman, Chem. Eur. J. 10 (2004) 3970.[4] M.A. Dewey, D.A. Knight, D.P. Klein, A.M. Arif, J.A. Gladysz, Inorg. Chem. 30
- [5] (a) M.A. Dewey, D.A. Knight, A. Arif, J.A. Gladysz, Chem. Ber. 125 (1992) 815; (b) M.A. Dewey, G.A. Stark, J.A. Gladysz, Organometallics 15 (1996) 4798.
- [6] W.R. Cantrell Jr., G.B. Richter-Addo, J.A. Gladysz, J. Organomet. Chem. 472 (1994) 195.
- [7] G.A. Stark, J.A. Gladysz, Inorg. Chim. Acta 269 (1998) 167.
- [8] (a) G.B. Richter-Addo, D.A. Knight, M.A. Dewey, A.M. Arif, J.A. Gladysz, J. Am. Chem. Soc. 115 (1993) 11863;
 - (b) G.A. Stark, M.A. Dewey, G.B. Richter-Addo, D.A. Knight, A.M. Arif, J.A. Gladysz, in: H. Werner, J. Sundermeyer (Eds.), Stereoselective Reactions of Metal-Activated Molecules, Vieweg-Verlag, Braunschweig, Germany, 1995, p.
- [9] (a) G.A. Stark, A.M. Arif, J.A. Gladysz, Organometallics 13 (1994) 4523; (b) T.J. Johnson, A.M. Arif, J.A. Gladysz, Organometallics 13 (1994) 3182.
- [10] For some well characterized examples and lead references, see (a) A.D. Garrett, P.S. White, J.L. Templeton, Inorg. Chim. Acta 361 (2008) 3135; (b) A.D. Garrett, N.J. Vogeley, J.R. Varner, P.S. White, J.L. Templeton,
- Organometallics 25 (2006) 1728. [11] L.J. Alvey, O. Delacroix, C. Wallner, O. Meyer, F. Hampel, S. Szafert, T. Lis, J.A. Gladysz, Organometallics 20 (2001) 3087.
- [12] For early reports of complexes of the formula L_nMCH₂NRR', see: (a) C.W. Fong, G. Wilkinson, J. Chem. Soc., Dalton Trans. (1975) 1100;
 - (b) D.J. Sepelak, C.G. Pierpont, E.K. Barefield, J.T. Budz, C.A. Poffenberg, J. Am. Chem. Soc. 98 (1976) 6178;
 - (c) E.K. Barefield, D.J. Sepelak, J. Am. Chem. Soc. 101 (1979) 6542; (d) D.H. Gibson, K. Owens, Organometallics 10 (1991) 1216.
- [13] For related phenomena involving phosphido complexes, see J. Giner Planas, F. Hampel, J.A. Gladysz, Chem. Eur. J. 11 (2005) 1402. [14] (a) W.C. Kaska, Coord. Chem. Rev. 48 (1983) 1;
- (b) H. Werner, W. Paul, R. Feser, R. Zolk, P. Thometzek, Chem. Ber. 118 (1985) 261;
- (c) G.C.A. Bellinger, H.B. Friedrich, J.R. Moss, J. Organomet. Chem. 366 (1989) 175.
- [15] (a) D. Basavaiah, A.J. Rao, T. Satyanarayana, Chem. Rev. 103 (2003) 811; (b) J.L. Methot, W.R. Roush, Adv. Synth. Catal. 346 (2004) 1035.
- [16] (a) A. Scherer, J.A. Gladysz, Tetrahedron Lett. 47 (2006) 6335;

 - (b) F. Seidel, J.A. Gladysz, Synlett (2007) 986; (c) F.O. Seidel, J.A. Gladysz, Adv. Synth. Catal. 350 (2008) 2443.
- S.N. Seidel, Doctoral Dissertation, Universität Erlangen-Nürnberg, 2009.
- [18] J.H. Merrifield, J.M. Fernández, W.E. Buhro, J.A. Gladysz, Inorg. Chem. 23 (1984) 4022.
- [19] (a) W.E. Buhro, B.D. Zwick, S. Georgiou, J.P. Hutchinson, J.A. Gladysz, J. Am. Chem. Soc 110 (1988) 2427:
 - (b) B.D. Zwick, M.A. Dewey, D.A. Knight, W.E. Buhro, A.M. Arif, J.A. Gladysz, Organometallics 11 (1992) 2673;
 - (c) M.A. Dewey, D.A. Knight, A.M. Arif, J.A. Gladysz, Z. Naturforsch., B.: Anorg. Chem., Org. Chem. 47 (1992) 1175; (d) D.A. Knight, M.A. Dewey, G.A. Stark, B.K. Bennett, A.M. Arif, J.A. Gladysz,
 - Organometallics 12 (1993) 4523: (e) P.C. Cagle, O. Meyer, K. Weickhardt, A.M. Arif, J.A. Gladysz, J. Am. Chem. Soc. 117 (1995) 11730;

- (f) P.C. Cagle, O. Meyer, D. Vichard, K. Weickhardt, A.M. Arif, J.A. Gladysz,
- Organometallics 15 (1996) 194. [20] F. Agbossou, E.J. O'Connor, C.M. Garner, N. Quirós Méndez, J.M. Fernández, A.T. Patton, J.A. Ramsden, J.A. Gladysz, Inorg. Synth. 29 (1992) 211.
- [21] W. Tam, G.-Y. Lin, W.-K. Wong, W.A. Kiel, V.K. Wong, J.A. Gladysz, J. Am. Chem. Soc. 104 (1982) 141.
- [22] J.H. Merrifield, G.-Y. Lin, W.A. Kiel, J.A. Gladysz, J. Am. Chem. Soc. 105 (1983) 5811.
- [23] J.H. Merrifield, C.E. Strouse, J.A. Gladysz, Organometallics 1 (1982) 1204.
- [24] The absolute configuration at rhenium is assigned according to the Baird–Sloan modification of the Cahn–Ingold–Prelog priority rules. The cyclopentadienyl is considered a pseudoatom of atomic number 30. This gives the following sequence: $\eta^5-C_5H_5>PPh_3>NO>NHRR',NRR',CH_2N.$ (a) K. Stanley, M.C. Baird, J. Am. Chem. Soc. 97 (1975) 6598; (b) T.E. Sloan, Top. Stereochem. 12 (1981) 1.
- [25] Representative examples from the literature: (a) D. Braga, S.L. Giaffreda, M. Polito, F. Grepioni, Eur. J. Inorg. Chem. (2005) 2737; (b) D.E. Janzen, M.E. Botros, G.P. Helton, D.G. Van Derveer, G.J. Grant, Acta Cryst. E62 (2006) o1550.
- [26] (a) C.P. Casey, M.A. Andrews, D.R. McAlister, J. Am. Chem. Soc. 101 (1979) 3371: (b) C.P. Casey, M.A. Andrews, D.R. McAlister, W.D. Jones, S.G. Harsy, J. Mol. Cat.
 - 13 (1981) 43.
- [27] (a) S. Georgiou, J.A. Gladysz, Tetrahedron 42 (1986) 1109; (b) S.G. Davies, I.M. Dordor-Hedgecock, K.H. Sutton, M. Whittaker, J. Am. Chem. Soc. 109 (1987) 5711.
- [28] J.A. Gladysz, B.J. Boone, Angew. Chem., Int. Ed. Engl. 36 (1997) 551. [29] R.H. Hoffmann, Angew. Chem. 112 (2000) 2134;
- R.H. Hoffmann, Angew. Chem. Int. Ed. 39 (2000) 2054.

- [30] Lead references: (a) J.W. Faller, B.V. Johnson, J. Organomet. Chem. 96 (1975) 99; (b) E. Bye, B.W. Schweizer, J.D. Dunitz, J. Am. Chem. Soc. 104 (1982) 5893; (c) H. Brunner, B. Hammer, C. Krüger, K. Angermund, I. Bernal, Organometallics

 - (d) S.G. Davies, A.E. Derome, J.P. McNally, J. Am. Chem. Soc. 113 (1991) 2854;
 - (e) J. Polowin, S.C. Mackie, M.C. Baird, Organometallics 11 (1992) 3724;
 - (f) S.E. Garner, A.G. Orpen, J. Chem. Soc., Dalton Trans. (1993) 533; (g) H. Brunner, R. Oeschey, B. Nuber, Angew. Chem., Int. Ed. Engl. 33 (1994) 866;
- H. Brunner, R. Oeschey, B. Nuber, Angew. Chem. 106 (1994) 941. [31] L. Duhamel, P. Duhamel, J.-C. Plaquevent, Tetrahedron: Asymmetry 15 (2004)
- [32] M. Prommesberger, Universität Erlangen-Nürnberg, unpublished results.
- [33] S. Eichenseher, Universität Erlangen-Nürnberg, unpublished results.
- [34] G.C. Fu, Acc. Chem. Res. 37 (2004) 542. [35] D.A. Castillo, F. Hampel, J.A. Gladysz, in preparation.
- [36] M.A. Dewey, J.A. Gladysz, Organometallics 12 (1993) 2390.
- [37] The quality of commercial Ph₃C⁺ X⁻ can vary, and crystallization from CH₂Cl₂/ hexanes or CH₂Cl₂/benzene is recommended, see: A.T. Patton, C.E. Strouse, C.B. Knobler, J.A. Gladysz, J. Am. Chem. Soc. 105 (1983) 5804.
- (a) B.V. Nonius "Collect" data collection software, 1998.; (b) Z. Otwinowski, W. Minor, "Scalepack" data processing software, in: Methods in Enzymology, Macromolecular Crystallography, Part A, vol. 276, 1997, p. 307.
- [39] G.M. Sheldrick, SHELX-97, Program for Refinement of Crystal Structures, University of Göttingen, 1997.
- [40] D.T. Cromer, J.T. Waber, in: J.A. Ibers, W.C. Hamilton (Eds.), International Tables for X-ray Crystallography, Kynoch, Birmingham, England, 1974. [41] H.D. Flack, Acta Cryst. A39 (1983) 876.